



This is to certify that the thesis entitled

THE EFFECT OF POSITIONAL SUBSTITUTION ON THE OPTICAL RESPONSE OF SYMMETRICALLY DISUBSTITUTED AZOBENZENE DERIVATIVES

presented by

Alexis Amon Blevins

has been accepted towards fulfillment of the requirements for the

Master of Science

Major Professor's Signature

Date

MSU is an Affirmative Action/Equal Opportunity Institution

PLACE IN RETURN BOX

to remove this checkout from your record.

TO AVOID FINES return on or before date due.

MAY BE RECALLED with earlier due date if requested.

DATE DUE	DATE DUE

11/00 c:/CIRC/DateDue.p65-p.33

THE EFFECT OF POSITIONAL SUBSTITUTION ON THE OPTICAL RESPONSE OF SYMMETRICALLY DISUBSTITUTED AZOBENZENE DERIVATIVES

By

Alexis Amon Blevins

A THESIS

Submitted to
Michigan State University
in partial fulfillment of the requirements
for the degree of

Master of Science

Department of Chemistry

2003

ABSTRACT

THE EFFECT OF POSITIONAL SUBSTITUTION ON THE OPTICAL RESPONSE OF SYMMETRICALLY DISUBSTITUTED AZOBENZENE DERIVATIVES

By

Alexis Amon Blevins

We report on the steady state and transient spectroscopy and characterization of a series *p*-diamido azobenzene compounds where the length of the amido substituents are varied in a regular manner. Of particular interest in these systems is the mechanism and energetics of the isomerization dynamics. Steady state spectroscopic results in conjunction with semi empirical modeling of isomerization in these systems reveals that the dominant ground state isomerization mechanism is transient rehybridization with the activation energy depending sensitively on the identity of the substituents. These results place limits on the utility of the azobenzenes for optical information storage applications.

ACKNOWLEDGMENTS

I would like to thank the Blanchard group for all of the help presented in completion of this study and the NSF for funding.

TABLE OF CONTENTS

Introduction	1
Chapter 1: Synthesis of Azobenzene Derivatives	9
Chapter 2: Calculations	29
Chapter 3: Time Resolved Spectroscopy	41
Conclusion	62
Appendix A: Mass Spectra of Compounds	66

LIST OF TABLES

Table 1. Reaction conditions and yield for synthesized compounds20
Table 2. Absorption maxima and molar absorptivities of azobenzene, <i>p</i> -diaminoazobenzene and the <i>p</i> -diamidoazobenzenes 1-5
Table 3. Transient optical decay functionalities and time constants of azobenzene, <i>p</i> -diaminoazobenzene and the <i>p</i> -diamidoazobenzenes 1-5 47

LIST OF FIGURES

Figure 1. Schematic of one possible layered polymer system for separations based on change in local free volume4
Figure 2. Isomerization mechanisms for azobenzene5
Figure 3. Calculation of change in position and spacing of azobenzene terminal groups, R, upon isomerization for both <i>meta</i> and <i>para</i> disubstituted azobenzene
Scheme 1. Synthetic route to disubstituted azobenzene14
Figure 4. Proton NMR spectrum of <i>p</i> -diamidoazobenzene before (middle) and after (bottom) recrystallization
Figure 5. Proton NMR spectrum of azobenzene17
Figure 6. Proton NMR spectrum of <i>p</i> -diaminoazobenzene18
Figure 7. Proton NMR spectrum of <i>p</i> -diamidoazobenzene18
Figure 8. Proton NMR spectra of a series of <i>p</i> -diamidoazobenzenes19
Figure 9. Absorbance spectrum of azobenzene26
Figure 10. Absorbance spectrum of <i>p</i> -diaminoazobenzene26
Figure 11. Absorbance spectra of azobenzene, <i>p</i> -diaminoazobenzene, and <i>p</i> -diamidoazobenzene27
Figure 12. Calculated energy levels and oscillator strengths for azobenzene, diaminoazobenzene, and diamidoazobenzene
Figure 13. Calculated isomerization surface for inversion mechanism of azobenzene
Figure 14. Calculated isomerization surface for rotation mechanism of azobenzene34
Figure 15. Calculated isomerization surface for inversion mechanism of <i>p</i> -diaminoazobenzene
Figure 16. Calculated isomerization surface for rotation mechanism of <i>p</i> -diaminoazobenzene36

Figure 17. Calculated isomerization surface for inversion mechanism of <i>p</i> -diamidoazobenzenediamidoazobenzene	.37
Figure 18. Calculated isomerization surface for rotation mechanism of <i>p</i> -diamidoazobenzene	.38
Figure 19. Possible experiment outcomes available in a transient absorbance experiment	.42
Figure 20. Transient absorbance response of a) azobenzene b) p -diaminoazobenzene c) p -diamidoazobenzene	.45
Figure 21. Transient absorbance response of two <i>p</i> -diamidoazobenzenes	.49
Figure 22. Absorbance spectrum of 5 upon varying durations of ultraviolet irradiation	52
Figure 23. Block diagram of UV/Visible instrument modification	.53
Figure 24. Example of an absorbance versus concentration graph used to determine molar absorptivity	.53
Figure 25. Recovery of the absorption due to the <i>trans</i> band in azobenzene at 318nm	
Figure 26. Recovery of the absorption due to the <i>trans</i> band in <i>p</i> -diaminoazobenzene at 370nm	.57
Figure 27. Recovery of the absorption due to the <i>trans</i> band in <i>p</i> -diamidoazobenzene at 370nm.	.58

LIST OF ABBREVIATIONS

Nuclear magnetic resonance is abbreviated as NMR.

Highest occupied molecular orbital is abbreviated as HOMO.

Lowest unoccupied molecular orbital is abbreviated as LUMO.

Dimethylsulfoxide is abbreviated as DMSO.

Tetrahydrofuran is abbreviated as THF.

INTRODUCTION

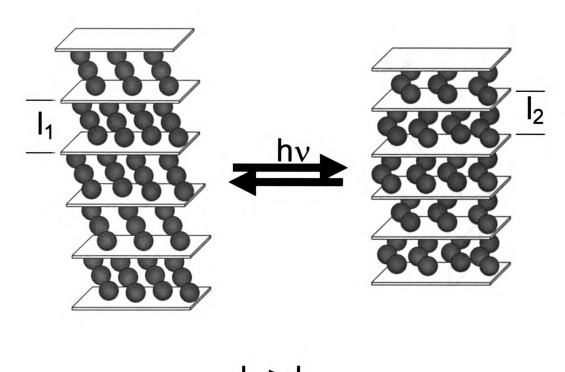
Azobenzenes are a family of compounds that has found wide use because of their facile photoisomerization and relatively high barrier to thermal (ground state) isomerization. These properties are of potential utility in the development of molecular-scale information storage and optical switching strategies.¹⁻¹¹ Among the key issues under investigation for the azobenzenes are the ability of substitution about their aromatic rings to mediate their optical properties and isomerization behavior. While it is typically assumed that the linear optical response and isomerization behavior of these chromophores is linked, this relationship has not been established. The purpose of this work is to examine how the presence of substituents on the azobenzene phenyl rings influences the spectroscopic and isomerization behavior of these compounds. We have synthesized a family of symmetrically para-disubstituted azobenzenes and have studied their steady state and time-resolved optical properties. We have also studied the branching ratio for isomerization and the rate of S₀ trans isomer recovery following photoisomerization for these species. Our findings indicate that the addition of substituents to the azobenzene chromophore can influence the steady state and time-resolved optical properties of the chromophore significantly, and the isomerization surfaces for these molecules are affected as well. This is not a surprising result because of the relationship between electronic structure and state ordering, and the electron density distribution for the bond(s) that dominate the isomerization coordinate. We understand this finding in the context of the N=N bond dominating the isomerization behavior of

these molecules, and the effective bond order of this moiety is influenced by the presence of electron-donating or electron-withdrawing substituents on the phenyl rings. Our finding that the isomerization barrier is reduced when electron-donating substituents are placed on the rings indicates that it is the π^* state that is influenced most strongly, and these findings are supported by the steady state spectra. Our data also point to the potential importance of asymmetric substitution of the azobenzene rings in structurally mediating isomerization.¹²

A secondary goal of this research was to evaluate substituted azobenzenes as interlayer polymer linkages. Using an isomerizable linkage, several applications may become feasible. In a layered polymer system it may be possible to both lock in the desired isomer and preserve the ability to switch to the alternative upon irradiation depending on the structure of the linkage and its concentration. Careful control of structure and concentration can lead to the eventual development of an optical storage device capable of both writing and erasing on a short time scale, where the "on" and "off" states have different absorbances and possibly different topography. The spectroscopic and physical changes of the polymer system allow for multiple methods of nondestructive reading of the information from the media. Another application that can be realized is the formation of a stacked polymer capable of separations based on size exclusion. Separations would work on the premise of a change in free volume of the polymer matrix due to the inter-layer linkage isomerization.(Figure 1) This scheme allows pore size and identity of polymer layers to be altered for chemical specificity independent of the separation based

exclusively on size. These two applications rely on the isomerization properties of an interlayer linkage, and we evaluate structured azobenzene derivatives with those goals in mind.

Until recently, the accepted model for the isomerization of azobenzenes was that there is a significant barrier to isomerization in the S₀ state, with the magnitude of the barrier being a consequence of the azo (N=N) moiety. We are not aware of an accurate determination of the thermal isomerization barrier for azobenzenes, either experimental or computational, but it has been thought to be on the order of ~50 kcal/mol and, because of this substantial energy, the modeling of this barrier cannot be done reliably using the usual assumption of a one-dimensional isomerization coordinate, i.e. both isomerization and ring rotation must be coordinated in some unresolved manner. When excited to the S₁ state, the azobenzene chromophore is thought to isomerize by an inversion, or rehybridization mechanism, and excitation to the S₂ state is thought to cause isomerization to proceed by rotation about the azo bond, which is taken to be substantially single-bond in character. 18 The two proposed mechanisms for azobenzene isomerization are illustrated in Figure 2. This widely accepted picture has continued to stir debate, owing to the relative timescales of large amplitude molecular motion and internal conversion from the S2 to the S1 manifold.



 $|_{1} > |_{2}$

Figure 1: Schematic of one possible layered polymer system for separations based on change in free volume.

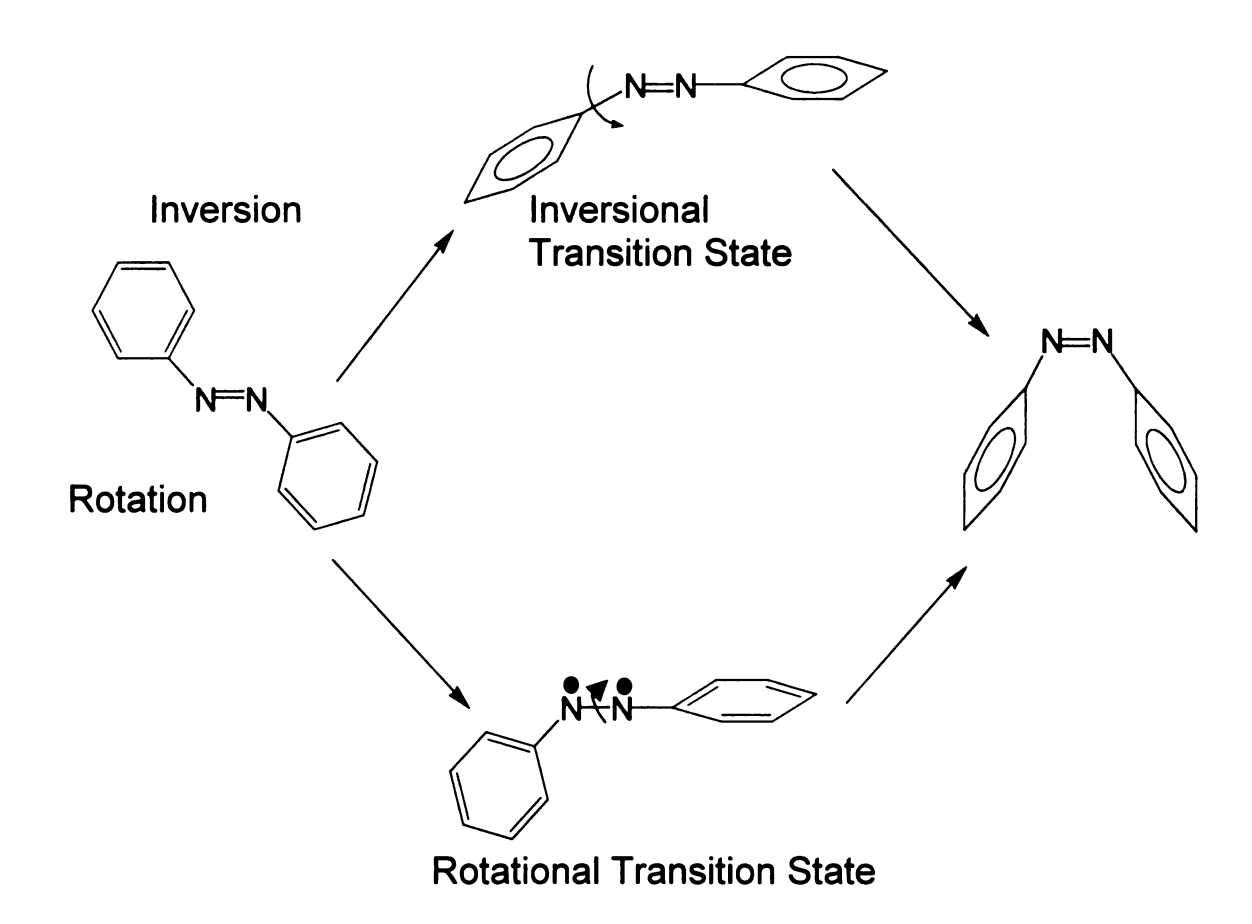


Figure 2: Isomerization mechanisms for azobenzene.

Recent elegant work by both the Tahara¹⁸ and Kobayashi¹⁹ groups has cast doubt on the "standard" picture. Using femtosecond optical techniques, Tahara's group has shown that excitation to the S₂ state of azobenzene undergoes rapid relaxation to the S₁ state, where isomerization proceeds.¹⁸ When viewed in the context of the characteristically short lifetime of highly excited electronic states in organic molecules, and the time required for inertial motion of the phenyl ring(s), these results are fully consistent with the behavior of most organic chromophores. The Kobayashi group, using chirped femtosecond pulses has demonstrated clearly that vibronic coupling is substantial in an excited azobenzene derivative and that the redistribution of energy within the vibrational manifold of the S₁ state serves to mediate the isomerization behavior of that species. 19 These findings on the earliest stages of relaxation within azobenzenes not only shed significant light on the factors mediating isomerization, they underscore the fact that a full understanding of isomerization in azobenzenes remains to be achieved.

With this background, we consider whether or not it is possible to mediate the isomerization behavior of azobenzenes by synthetic means. We are interested in being able to incorporate *p*-disubstituted azobenzenes into layered assemblies for the purposes of probing local structure using isomerization and for determining whether or not a layered structural motif is capable of storing information via optical read/write means. In an attempt to address these issues, we have focused on the synthesis and characterization of a family of simple *p*-disubstituted azobenzenes, with particular interest in the influence of the *para*

disubstitution on the spectroscopic and isomerization behavior of the resulting chromophores. The compounds studied are structurally simplified models for disubstituted species capable of layer incorporation. We consider the experimental spectroscopic and calculated isomerization results separately.

Literature Cited

- 1. Saremi, F.; Tieke, B. Adv. Mater., 1998, 10, 388.
- 2. Wang, C.; Fei, H.; Xia, J.; Yang, Y.; Wei, Z.; Yang, Q.; Sun, G. *Appl. Phys. B.*, **1999**, *68*, 1117.
- 3. Howe, L. A.; Jaycox, G. D. J. Poly. Sci. A. Poly. Chem., 1998, 36, 2827.
- 4. Yoshii, K.; Machida, S.; Horie, K. J. Poly. Sci. B. Poly. Phys., 2000, 38, 3098.
- 5. Aoshima, Y.; Egami, C.; Kawata, Y.; Sugihara, O.; Tsuchimori, M.; Watanabe, O.; Fugimara, H.; Okamoto, N. *Polym. Adv. Tech.*, **2000**, *11*, 575.
- 6. Zilker, S. J.; Bieringer, T.; Haarer, D.; Stein, R. S.; van Egmond, J. W.; Kostromine, S. G. *Adv. Mater.*, **1998**, *10*, 855.
- 7. Eicher, J. J.; Orlic, S.; Schulz, R.; Rubner, J. Opt. Lett., 2001, 26, 581.
- 8. Hagen, R.; Bieringer, T. Adv. Mater., 2001, 13, 1805.
- 9. Pedersen, T. G.; Johansen, P. M.; Pedersen, H. C. *J. Opt. A: Pure Appl. Opt.*, **2000**, *2*, 272.
- 10. Patane, S.; Arena, A.; Allegrini, M.; Andreozzi, L.; Faetti, M.; Giordano, M. Opt. Commun., 2002, 210, 37.
- 11. Astrand, P.-O.; Ramanujam, P. S.; Hvilsted, S.; Bak, K. L.; Suauer, S. P. A. *J. Am. Chem. Soc.*, **2000**, *122*, 3482.
- 12. Tamada, K.; Akiyama, H.; Wei, T.-X.; Kim, S.-A. Langmiur, 2003, 19, 2306.
- 13. Fujino, T.; Arzhantsev, S. Y.; Tahara, T. *J. Phys. Chem. A*, **2001**, *105*, 8123.
- 14. Saito, T.; Kobayashi, T. J. Phys. Chem. A, 2002, 106, 9436.

Chapter 1

SYNTHESIS OF AZOBENZENE DERIVATIVES

A switching application in a polymer matrix requires that the molecule undergoing the switching operation needs to have significant local freedom. This freedom can be achieved many ways; through careful selection of a molecule's synthetic substitution and control on concentration in the matrix most of the freedom can be achieved. We are exploring the use of azobenzene in a layered polymer matrix. Photoisomerization of the azobenzene moiety gives rise to spectral shifts, and this family of molecules has been evaluated for photochromic optical switching by other groups. 1-6 The meta and para-disubstituted varieties of azobenzene are the most useful to evaluate due to the feasibility of their incorporation in polymer side groups through functionalized substituents. The position of the functionalized substituents on the azobenzene ring greatly affects the overall molecular length and thus the degree of change in free volume of the polymer matrix. Calculations conducted in Hyperchem® v. 6.0 show that the distance differential (Figure 3) for the meta-disubstituted species upon isomerization is approximately 1.1 Å. The same process for the paradisubstituted species yields a change of 5.5 Å. This leads to the incorporation of the meta-disubstituted azobenzene as the switching molecule due to reduced strain on the molecule.(Figure 3)

Figure 3: Calculation of change in position and spacing of azobenzene terminal groups, R, upon isomerization for both *meta* and *para* disubstituted azobenzene.

The synthesis of substituted azobenzenes, of necessity, requires reactions targeted to specific ring positions. Any of the ring substituents used in the reactions acts as an ortho, para-director and a meta deactivator. There are a number of possible ways to overcome this issue. The first is to place a substituent on the ortho position relative to the azo nitrogen that directs further addition to the *meta* position. This however limits the molecular variety that can be employed and may have significant steric consequences on the efficiency and speed of photoisomerization. Another possibility is to start with substituted anilines and form the azo bond as the final step. Forming the azo bond as the last step becomes a major problem as the connectivity to the polymer must be considered before the molecule can be planned, and swing to the metadeactivation behavior of the azo moiety, subsequent loss of meta substituents is a common result. Most of the connections to polymer sheets considered for the azobenzene were of the covalent type that the Blanchard group has extensive experience. The overall difficulty of *meta*-disubstituted azobenzene synthesis lead to the selection of the para disubstituted molecules for the isomerization studies.

As mentioned previously the *para*-disubstituted azobenzenes lack the structural freedom that is desired for facile isomerization in a lamellar environment. To a limited degree the lack of freedom can be overcome by only connecting one side of the molecule to the polymer sheets. Singular connectivity has been evaluated by other groups by incorporating functionalized azobenzenes in poly(methyl-methacralate) matrices in a "doping" procedure.⁵⁻⁸ While doping

makes optical storage possible and simultaneously provides a probe into local chemical environment, it limits the overall usefulness of the devices. Providing connectivity at each end of the molecule affords higher durability and increased degree of order, which nearly directly correlates to overall increased switching cycles before degradation. With that, the para-disubstituted azobenzene needed to be functionalized with a moiety that has enough structural freedom to accommodate the steric limitations of p-disubstituted azobenzene. Alkane chains have many degrees of freedom, which can be used to accommodate structural changes. In addition alkane chains are relatively inert and allow for simple polarity modulated processes to be employed in the purification of the synthesized molecule. We decided that starting with a diaminoazobenzene the alkane chain could be attached through an amide functionality. We anticipated that the attachment of anything to the azobenzene ring(s) would influence its optical response, but theoretical predictions of these changes are not reliable. The ability to connect to the interlayer moieties will eventually need to be introduced on the ring of the azobenzene para to the azo bond but a model study of this family of azobenzenes was conducted first to evaluate the effect of ring substitution on the optical and isomerization properties of this family of chromophores.

The series of *p*-diamidoazobenzenes we report on here were synthesized using a modification of a standard polyamido polymerization route.⁹ We have replaced the dicarboxylic acid with a monofunctional acid chloride to prevent polymerization. The reaction is illustrated in Scheme 1. 4,4'-Azodianiline was

purchased from Sigma-Aldrich (CAS 538-41-0). The reactions were carried out under an inert atmosphere to limit hydrolysis of the acid chloride. Methylene chloride, acetone and tetrahydrofuran were purchased from Sigma-Aldrich and used as received. N-methylmorpholine was used to scavenge hydrochloric acid produced during the reaction. Reaction times of thirty minutes at room temperature were typical, with little or no increase in yield for longer reaction times. Typical reaction conditions were for 2 mmol of 4,4'-azodianiline to be combined with 8 mmol of N-methylmorpholine and 8 mmol of the appropriate acid chloride in 150 mL of CH₂Cl₂. Following completion of the reaction, the solution was washed with 150 mL of 2M HCl. The diamidoazobenzene precipitated from solution along with the appropriate acid byproduct and was collected by filtration. The resulting solid was dissolved in acetone and washed with an equal volume of brine solution (saturated NaCl) to separate the derivatized azobenzene from the acid reaction byproducts, and the crude product was then separated from the acetone. The solid was purified by recrystallization from methanol/water (80:20). As the alkyl substituent of the acid chloride increased in length, the purity of the p-diamidoazobenzene product could be increased significantly by additional washing with brine solution. The reaction to synthesize 5 produced lower yields due to the nonpolar nature of the product. For this reaction THF was used in place of CH₂Cl₂ as the solvent due to the limited solubility of nonanoyl chloride in CH₂Cl₂. The use of THF as the solvent required a methanol washing of the recovered solid to remove unreacted starting materials, but eliminated the need for recrystallization. Purity of the

Scheme 1: Synthetic route to disubstituted azobenzene.

compounds synthesized was determined by proton NMR and UV/Visible spectroscopy. Figure 4 shows the progression from starting material (top) to final product (bottom) showing an impure substance (middle). Mass spectra were taken for each of the products and can be found in Appendix A.

The NMR spectra reported here were obtained on a Varian 300 MHz instrument using a standard proton collection method. The proton NMR spectrum of azobenzene demonstrates two groupings of protons at about 7.5, and 7.9 ppm. These groupings represent all the protons on the phenyl rings of the azobenzene and are split according to Figure 5. The addition of the amine groups further splits the phenyl protons to 6.5 and 7.9 ppm and should add an additional peak to represent the amine protons; however this has never been experimentally seen. (Figure 6) The conversion to the amide removes one of the amine protons and replaces it with alkyl protons which are seen in the spectrum. As the alkyl chain is extended the shift of the amide proton is unaffected and additional peaks appear in the aliphatic region (δ 0.6 to 1.6 ppm) of the spectrum to correspond with the additional methylenes. (Figure 7 and Figure 8) The associated proton shifts, synthetic yields, and general descriptions for the compounds are presented below. The reaction conditions and yields are presented in Table 1.

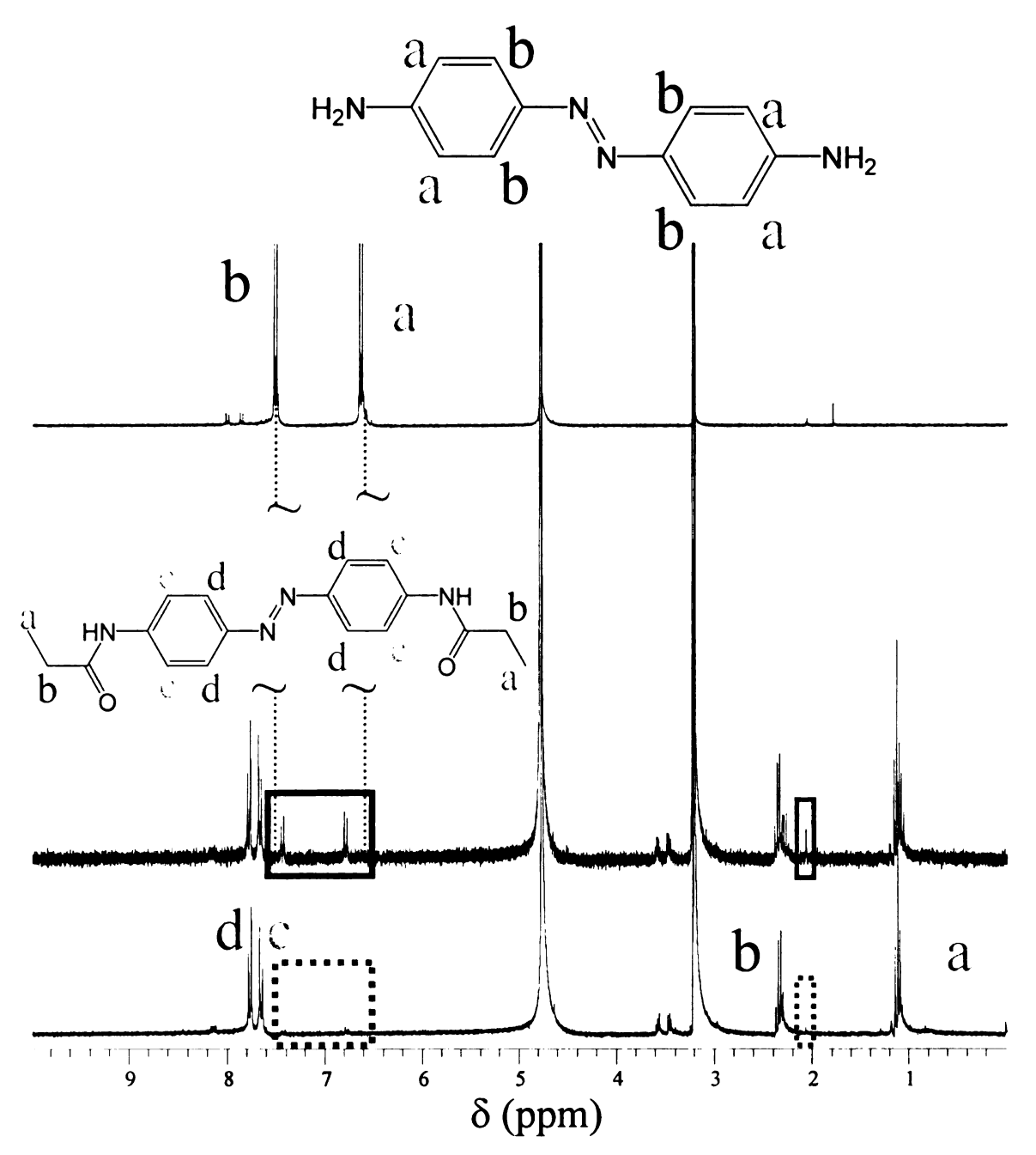


Figure 4: Proton NMR spectrum of *p*-diaminoazobenzene (top), *p*-diamidoazobenzene before (middle) and after (bottom) recrystallization.

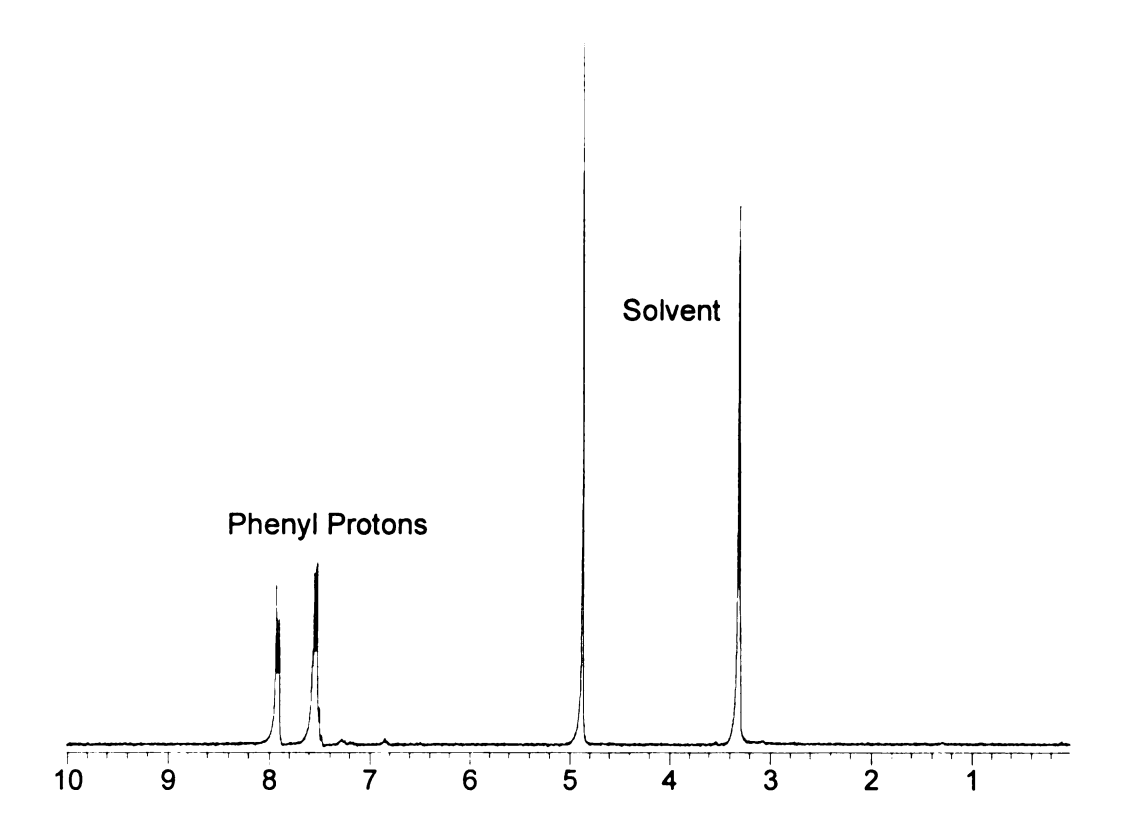
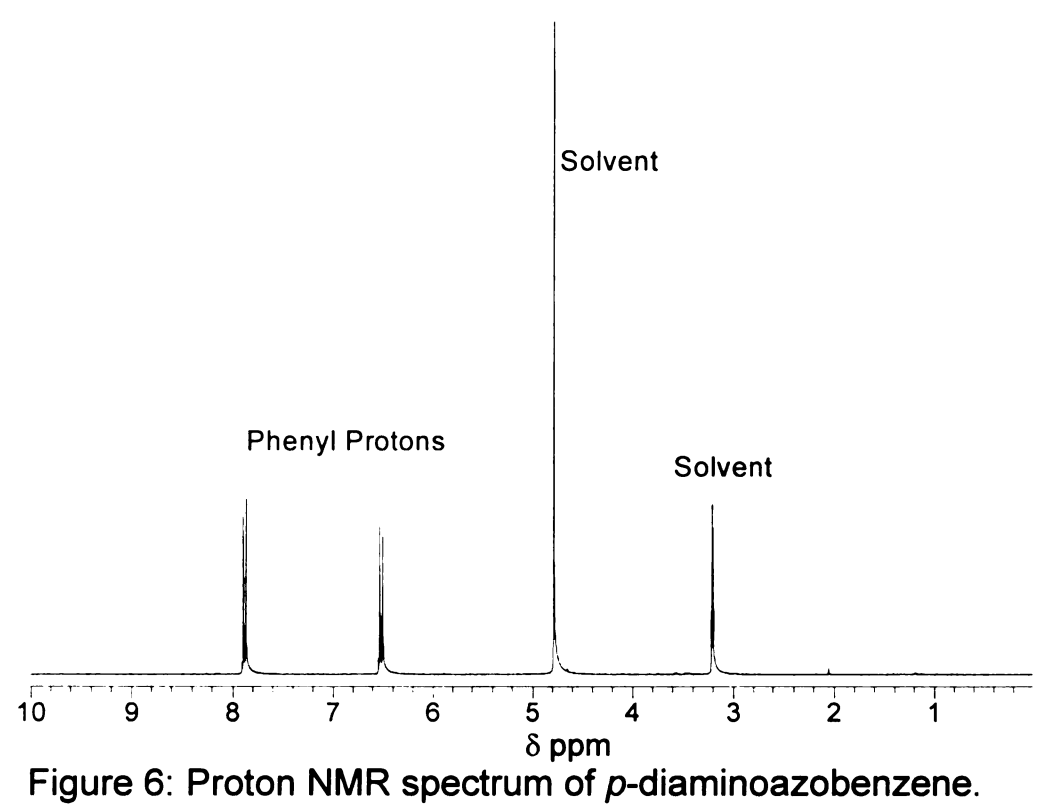


Figure 5: NMR spectrum of azobenzene in deuterated methanol.



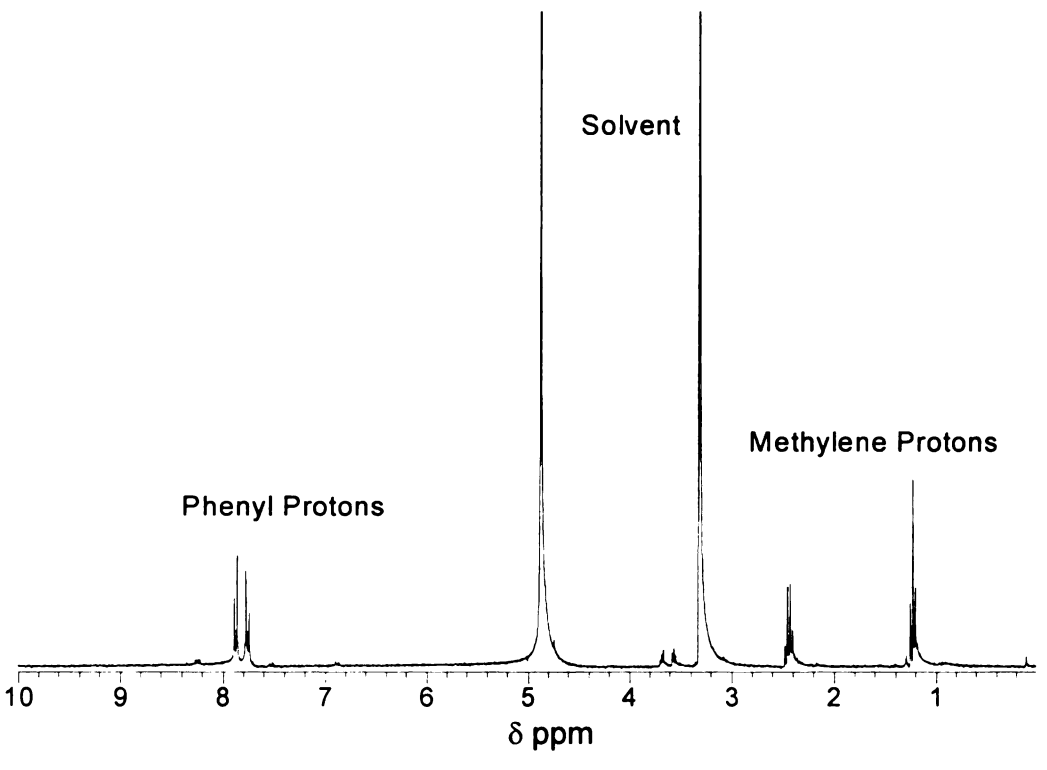


Figure 7: Proton NMR spectrum of *p*-diamidoazobenzene.

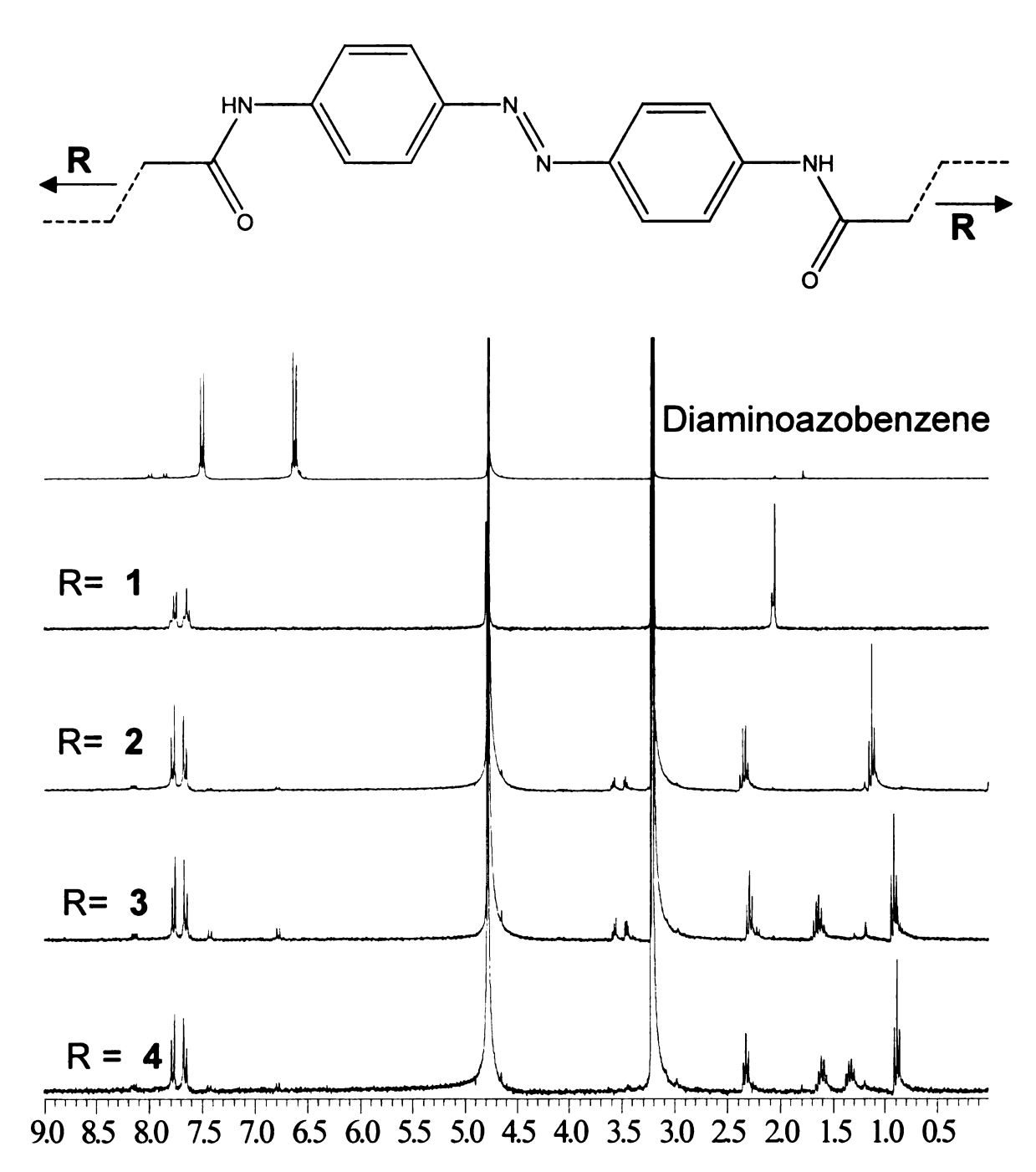


Figure 8: NMR spectra of a series of *p*-diamidoazobenzenes.

Reaction Conditions / Results					
Compound	Time Stirred (min)	Solvent	Crude Yield	Recrystallized Yield	
1	28	CH ₂ Cl ₂	80%	53%	
2	28	CH ₂ Cl ₂	73%	54%	
3	30	CH₂Cl₂	46%	44%	
4	28	CH₂Cl₂	34%	30%	
5	40	THF	69%	No Recrystallization	

Table 1 : Reaction conditions and yield for synthesized compounds.

Compound 1. (N-[4-(4-Acetylamino-phenylazo)-phenyl]-acetamide) This compound was produced with a crude yield of 80% and recrystallized yield of 53% using CH₂Cl₂ as reaction solvent. The resulting brown flakes showed proton NMR peaks (300 MHz, *d*-methanol) at δ: 2.14 ppm (s, 6H alkyl protons), 7.70 ppm (m, 4H on benzene ring), and 7.90 ppm (m, 4H on benzene ring). The mass spectrum (GC/MS) of the compound showed peaks at m/z 43, 65, 92, 134, 162, and 296.

Compound 2. (*N*-[4-(4-Propionylamino-phenylazo)-phenyl]-propionamide) This compound was produced with a crude yield of 73% and recrystallized yield of 54% using CH_2CI_2 as reaction solvent. The resulting brown flakes showed proton NMR peaks (300 MHz, *d*-methanol) at δ : 1.22 ppm (m, 6H β to carbonyl), 2.44ppm (m, 4H α to carbonyl), 7.77 ppm (m, 4H on benzene ring), and 7.87 ppm (m, 4H on benzene ring). The mass spectrum (GC/MS) of the compound showed peaks at m/z 57, 92, 119, 148, 149, 176, 324, 325.

Compound 3. (*N*-[4-(4-Butyrylamino-phenylazo)-phenyl]-butyramide) This compound was produced with a crude yield of 46% and recrystallized yield of 44% using CH₂Cl₂ as reaction solvent. The resulting orange needles showed proton NMR peaks (300 MHz, *d*-methanol) at δ : 0.92 ppm (m, 6H γ to carbonyl), 1.63 ppm (m, 4H β to carbonyl), 2.29 ppm (m, 4H α to carbonyl), 7.70 ppm (m, 4H on benzene ring), and 7.90 ppm (m, 4H on benzene ring). The mass spectrum (GC/MS) of the compound showed peaks at m/z 43, 71, 92, 120, 162, 190, 211, 282, 352, and 353.

Compound 4. (Pentanoic acid [4-(4-pentanoylamino-phenylazo)-phenyl]-amide) This compound was produced with a crude yield of 34% and recrystallized yield of 30% using CH_2Cl_2 as reaction solvent. The resulting orange powder showed proton NMR peaks (300 MHz, *d*-methanol) at δ: 0.89 ppm (m, 6H δ to carbonyl), 1.32 ppm (m, 4H γ to carbonyl), 1.61 ppm (m, 4H β to carbonyl), 2.33 ppm (m, 4H α to carbonyl), 7.67 ppm (m, 4H on benzene ring), and 7.78 ppm (m, 4H on benzene ring). The mass spectrum (GC/MS) of the compound showed peaks at m/z 57, 92, 120, 176, 211, 296, 380, and 381.

Compound 5. (Nonanoic acid [4-(4-nonanoylamino-phenylazo)-phenyl]-amide) This compound was produced with a crude yield of 69% using THF solvent and no recrystallization was performed. The resulting yellow powder showed proton NMR peaks (300 MHz, *d*-dimethylsulfoxide) at δ : 0.85 ppm (d, 6H ι to carbonyl), 1.25 ppm (m; 20H η , ϕ , ϵ , δ , and γ to carbonyl), 1.55 ppm (m, 4H β to carbonyl), 2.33 ppm (m, 4H α to carbonyl), 6.81 ppm (d, 4H on benzene ring), 7.52 ppm (d, 4H on benzene ring), and 7.81 ppm (s, amide proton). The mass spectrum (GC/MS) of the compound showed peaks at m/z 43, 108, 120, 211, 232, 352, 490, and 492.

The absorbance spectra of the various azobenzenes reported here were obtained on a Varian/Cary model 300 UV/Visible absorption spectrometer.

Spectral resolution for all measurements was 1 nm. The molar absorptivities and absorption maxima of the compounds are given in Table 2.

Compound	Absorption maximum (nm)	ε _{max} (L/mol-cm)	ε ₄₅₀ (L/mol-cm)
Azobenzene	313	22400	500
<i>p</i> - diaminoazobenzene	394	27800	1630
1	364	17900	1300
2	364	23750	2400
3	364	24200	2530
4	364	24900	2500
5	364	25300	2450

Table 2. Absorption maxima and molar absorptivities of azobenzene, p-diaminoazobenzene and the p-diamidoazobenzenes 1-5.

The steady state absorption spectroscopy of azobenzene is well understood. The $S_1 \leftarrow S_0$ transitions for both the *trans* and *cis* forms are characterized by weak absorption bands ($\varepsilon \sim 500$ L/mol-cm for cis, $\varepsilon \sim 2,000$ L/mol-cm for trans), and these bands are centered at ~ 434 nm. The $S_2 \leftarrow S_0$ absorption bands for both isomers are stronger, with the trans band at 313 nm (e ~ 22,400 L/mol-cm) and the cis band at 254 nm (ϵ ~ 12,000 L/mol-cm). ¹⁰⁻¹² The addition of amino groups at the para positions causes a substantial change in the absorption spectrum. For p-diaminoazobenzene, the dominant absorption band is at ~ 420 nm (ε = 22,800 L/mol-cm), with weaker bands seen at 310 nm and 250 nm. The spectra can be seen in Figures 9,10, and 11. For the solution phase spectra we recorded, we did not attempt to isolate *cis* and *trans* conformers, so it is not clear based on the experimental data if the bands at 310 nm and 250 nm correspond to trans and cis forms, respectively, or if these bands represent two different excited electronic states of the same (presumably trans) conformer. This remarkable change in the absorption spectra resulting from para disubstitution reflects a change in the electronic excited state(s), and this is seen in the results of semi-empirical calculations for both cis and trans conformers (Figure 12), where the dominant absorption transition ($S_2 \leftarrow S_0$) is seen to redshift by $\sim 7000 \text{ cm}^{-1}$ upon addition of the p-amino functionalities. Reaction of the diamino functionalities to produce the p-diamido azobenzene derivatives produces a blue-shifted absorption band relative to the p-diamino compound. The experimental spectra can be reconciled with the results of semi-empirical calculations for both conformers (Figure 12), and for all of the azobenzenes, it

appears that multiple $S_n \leftarrow S_0$ transitions contribute significantly to the observed linear optical response. While the spectral red shift seen for diamidoazobenzenes relative to diaminoazobenzenes may appear to violate one's intuition, we believe that these findings are the result of changes in transition oscillator strength of low lying transitions with the addition of amido substituents rather than actual band shifts. Both experimental data and semi-empirical calculations point to the significant substituent-dependence of the electronic state energies of the azobenzenes.

A series of *p*-diamidoazobenzenes was synthesized according to Scheme 1 using a classic polymerization route relatively high yields and purity. The *para* position was selected for substitution due to ease of synthesis. The purity of the synthesis was checked by proton NMR and it was found that with increased alkyl chain length of the amide substituent additional peaks appeared in the aliphatic region of the spectrum. It was found that all of the *p*-diamidoazobenzenes have identical absorbance maxima suggesting that the electronic states of the compounds are identical. This absorbance maximum differs from that for *p*-diaminoazobenzene and that of azobenzene, suggesting that electronic states of the three compounds are quite different. This difference was the motivation for a series of calculations to model the isomerization of the molecules.

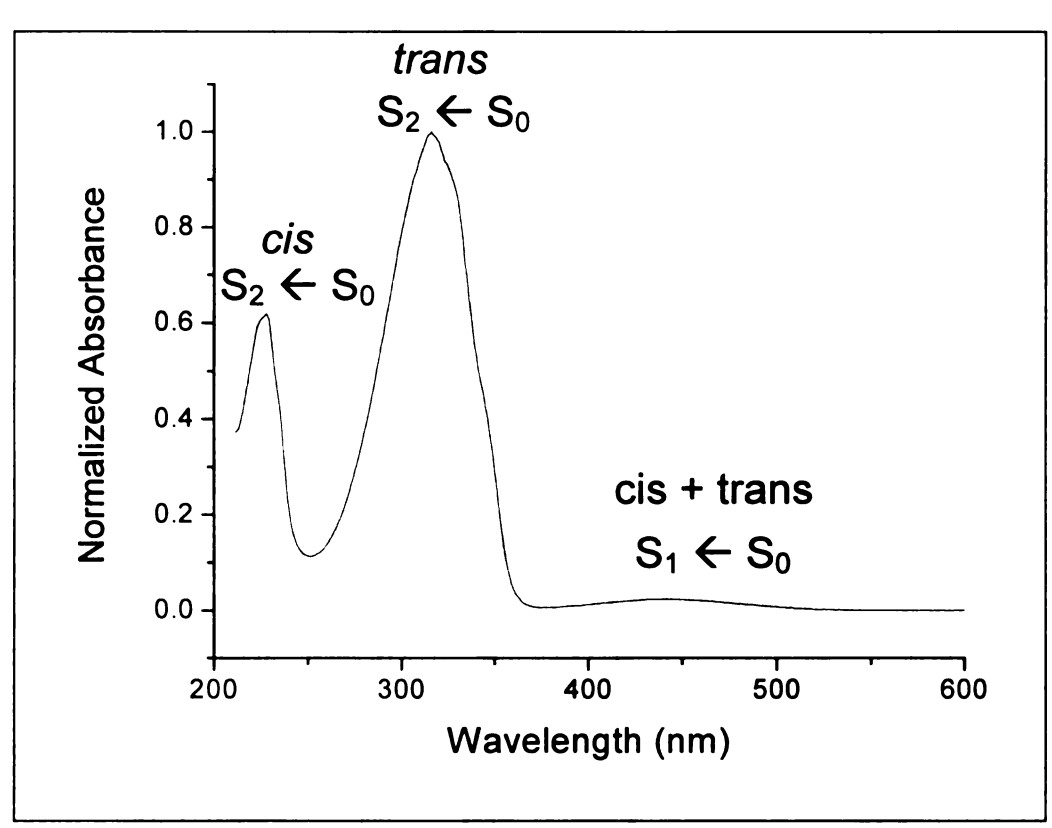


Figure 9: Absorbance spectrum of azobenzene.

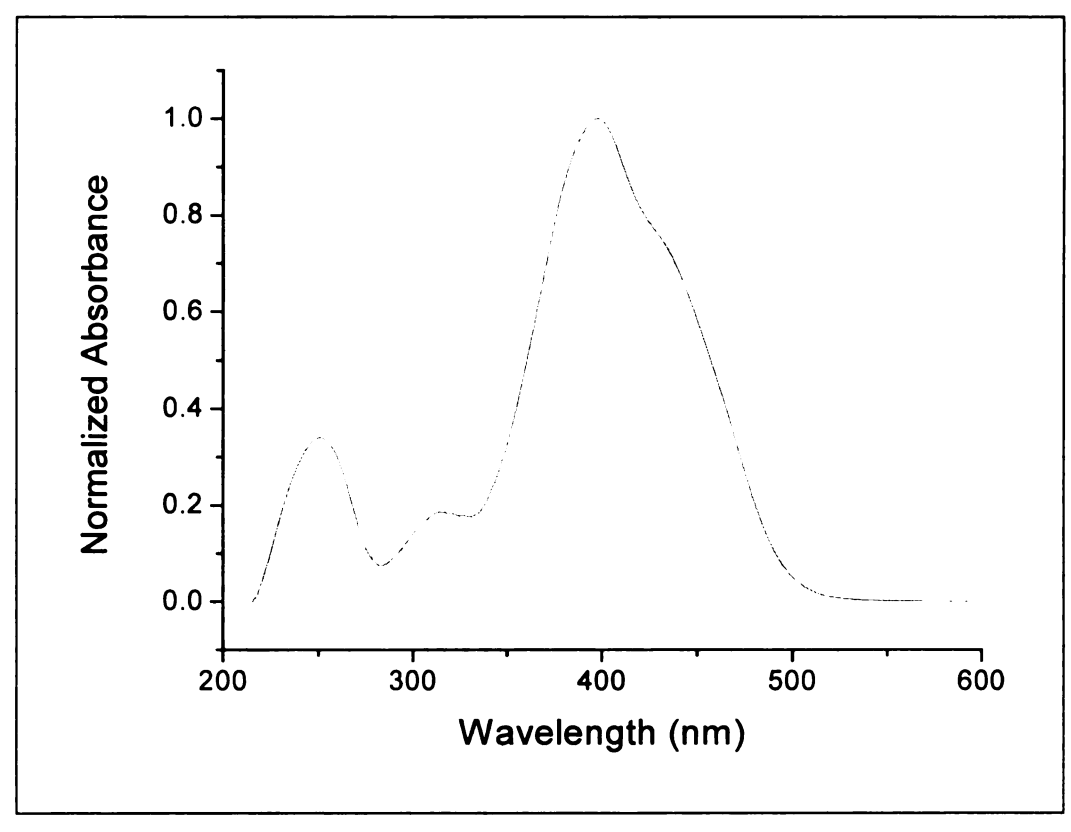


Figure 10: Absorbance spectrum of *p*-diaminoazobenzene.

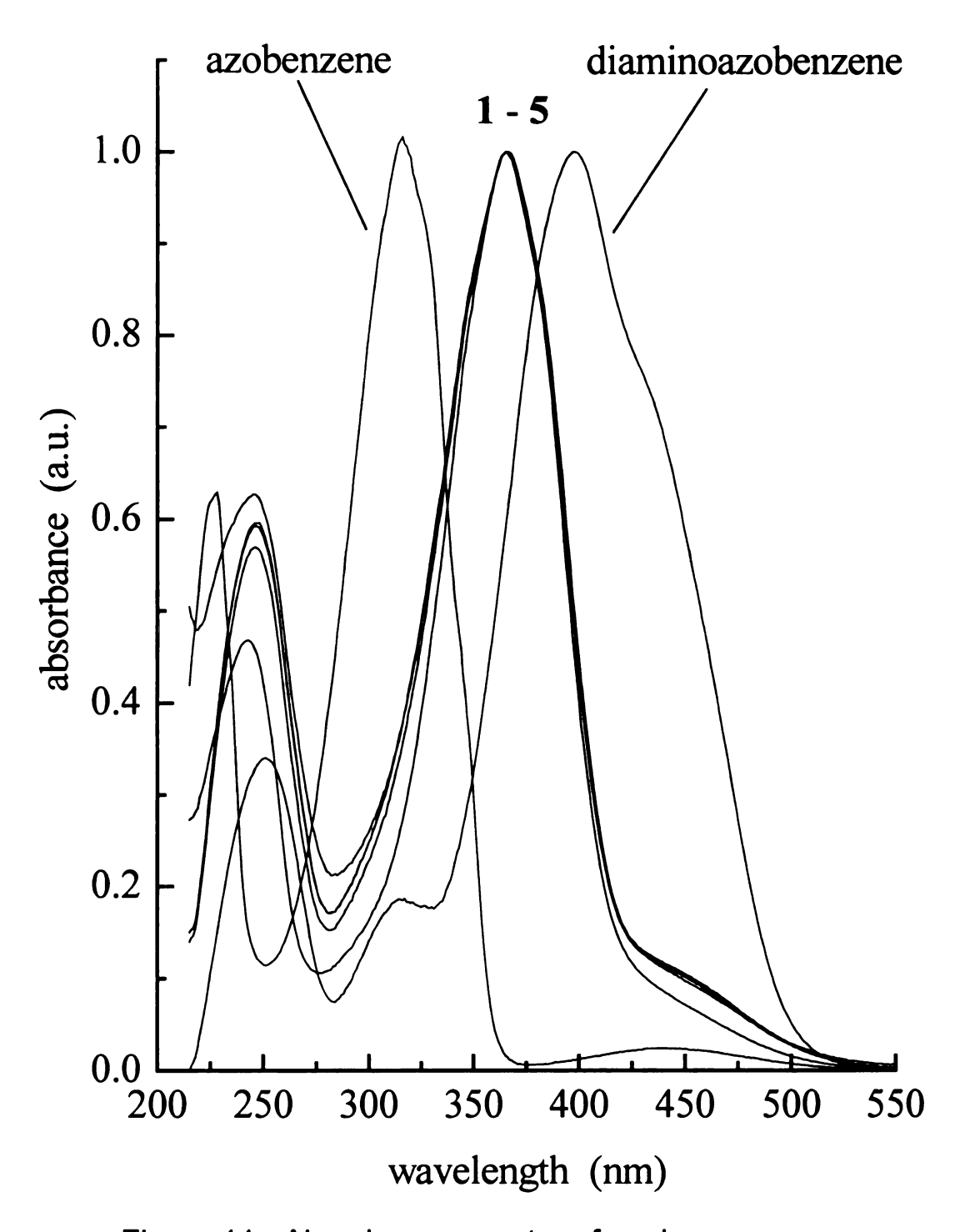


Figure 11 : Absorbance spectra of azobenzene, *p*-diaminoazobenzene, and *p*-diamidoazobenzene.

Literature Cited

- 1. Howe, L. A.; Jaycox, G. D. J. Poly. Sci. A. Poly. Chem., 1998, 36, 2827.
- 2. Saremi, F.; Tieke, B. Adv. Mater., 1998, 10, 388.
- 3. Ruslim, C.; Ichimura, K. J. Mater. Chem., 1999, 9, 673.
- 4. Delaire, J. A.; Nakatani, K. Chem. Rev., 2000, 100, 1817.
- 5. Badjic, J. D.; Kostic, N. M. J. Mater. Chem., 2001, 11, 408.
- 6. Seki, T.; Fukuchi, T.; Ichimura, K. Langmuir, 2002, 18, 5462.
- 7. Patane, S.; Arena, A.; Allegrini, M.; Andreozzi, L.; Faetti, M.; Giordano, M. Opt. Commun., 2002, 210, 37.
- 8. Hagen, R.; Bieringer, T. Adv. Mater., 2001, 13, 1805.
- 9. Misra, G. S. *Introductory Polymer Chemistry*; Wiley Eastern Limited: New Delhi, India, 1993.
- Lednev, I. K.; Ye, T.-Q.; Matousek, P.; Towrie, M.; Foggi, P.; Neuwahl, F. V. R.; Umapathy, S.; Hester, R. E.; Moore, J. N. Chem. Phys. Lett., 1998, 290, 68.
- 11. Lednev, I. K.; Ye, T.-Q.; Abbott, L. C.; Hester, R. E.; Moore, J. N. *J. Phys. Chem. A*, **1998**, *102*, 9161.
- 12. Zimmerman, G.; Chow, L. Y.; Paik, U. J. J. Am. Chem. Soc., 1958, 80, 3528.

Chapter 2

CALCULATIONS

Modeling azobenzenes at the semi-empirical level is a difficult undertaking due primarily to the presence of the poorly parameterized –N=N- functionality. Ideally the perfect model of a compound would take into account every aspect of said molecule and the interactions with the surroundings. The closest to this ideal at the current time is to perform a series of ab initio calculations. These calculations model the π -electrons and all of the bonds. The problem with ab initio calculations is that they require large amounts of processing power and time. In the case of azobenzene, the conjugated π-system actually lends itself well to parameterization and timescale of the ab initio calculation lengthens unacceptably. One alternative to ab initio studies is to perform semi-empirical^{1,2} calculations. These calculations only take into account the π -electrons and, as such, require that many assumptions be made. The π-system and bond motions are both parameterized and inserted into the equation in a semi-empirical calculation, where as they would be generated by the calculation itself in an ab initio experiment. Both methods require that the lowest energy conformer of the molecule be determined and used as the starting point. Semi-empirical calculations were performed on a Windows-based PC using Hyperchem® v. 6.0. Dihedral angles were incremented for isomerization barrier calculations using macros written in Microsoft Excel[®]. For these calculations, initial geometry optimization was performed using PM3 parameterization, then single point

calculations were made for the molecule at each incremented angle without additional geometry optimization. For calculations at the optimized S₀ geometry we report energy levels and oscillator strengths for *cis* and *trans* conformers (Figure 12). Based on these stepped geometry calculations, the isomerization surfaces for azobenzene have been calculated and are presented in Figures 13 thru 18.

We have attempted the calculation of the isomerization surfaces for the substituted azobenzenes, and we find that semi-empirical calculations do not reflect the experimental substituent-dependence on back isomerization barrier height. This is not surprising given the parameterization used in semi-empirical calculations and the multidimensional nature of the isomerization coordinate for azobenzenes. Even with the limitations of such calculations, we can extract useful information from them. Many groups have evaluated the isomerization process for azobenzene. Most groups have primarily concentrated on the conversion from the S₂ state to the ground state.^{3,4} One issue that has not been addressed is the mechanism of ground state (thermal) isomerization for this class of molecules. Our calculations for azobenzene, presented in Figures 13 and 14, show the calculated energy surfaces for the S_0 (a) and S_1 (b) states, for isomerization by rehybridization of one N (Figure 13) or rotation about the N=N bond (Figure 14). These calculated results predict that (thermal) isomerization in the ground state proceeds by rehybridization and not by -N=N- bond rotation. We calculate a $cis \rightarrow trans$ barrier height of 33 kcal/mol for S₀ rehybridization, compared to a 48 kcal/mol barrier for S₀ ring rotation. When comparing the

calculated results for isomerization on the S_0 and S_1 surfaces, a relatively small S_1 barrier is indicated for rehybridization (~ 12 kcal/mol), and the S_1 surface is calculated to be barrierless for ring rotation. While it is tempting to use this information to infer the dominance of N=N rotation as the primary isomerization coordinate in the S_1 , we do not feel justified in making this conclusion because an almost barrierless isomerization pathway can be traced out on either surface provided the ring rotation coordinate has sufficient time to locate the minimum on the S_1 surface prior to relaxation back to the S_0 surface. These calculated results should be taken as an indication of the substantially more facile nature of isomerization on the S_1 surface than is possible on the S_0 surface for azobenzene.

Corresponding calculations were conducted on both the *p*-diaminoazobenzene and *p*-diamidoazobenzene and are presented in Figures 15, 16, 17, and 18. In Figure 16 the region of high energy is due to a calculational error and is not representative of the real molecule. It is remarkable that both the inversion and rotation mechanism calculations yield nearly identical results for azobenzene, *p*-diaminoazobenzene, and *p*-diamidoazobenzene. This similarity suggests that substitution at the *para* position on the molecule has little to no effect on the isomerization. It is believed that similar calculations on a series of *meta* substituted azobenzenes would yield differentiated surfaces due to the interference of the substituent with the rotation mechanism. This interaction is removed by *para* substitution.

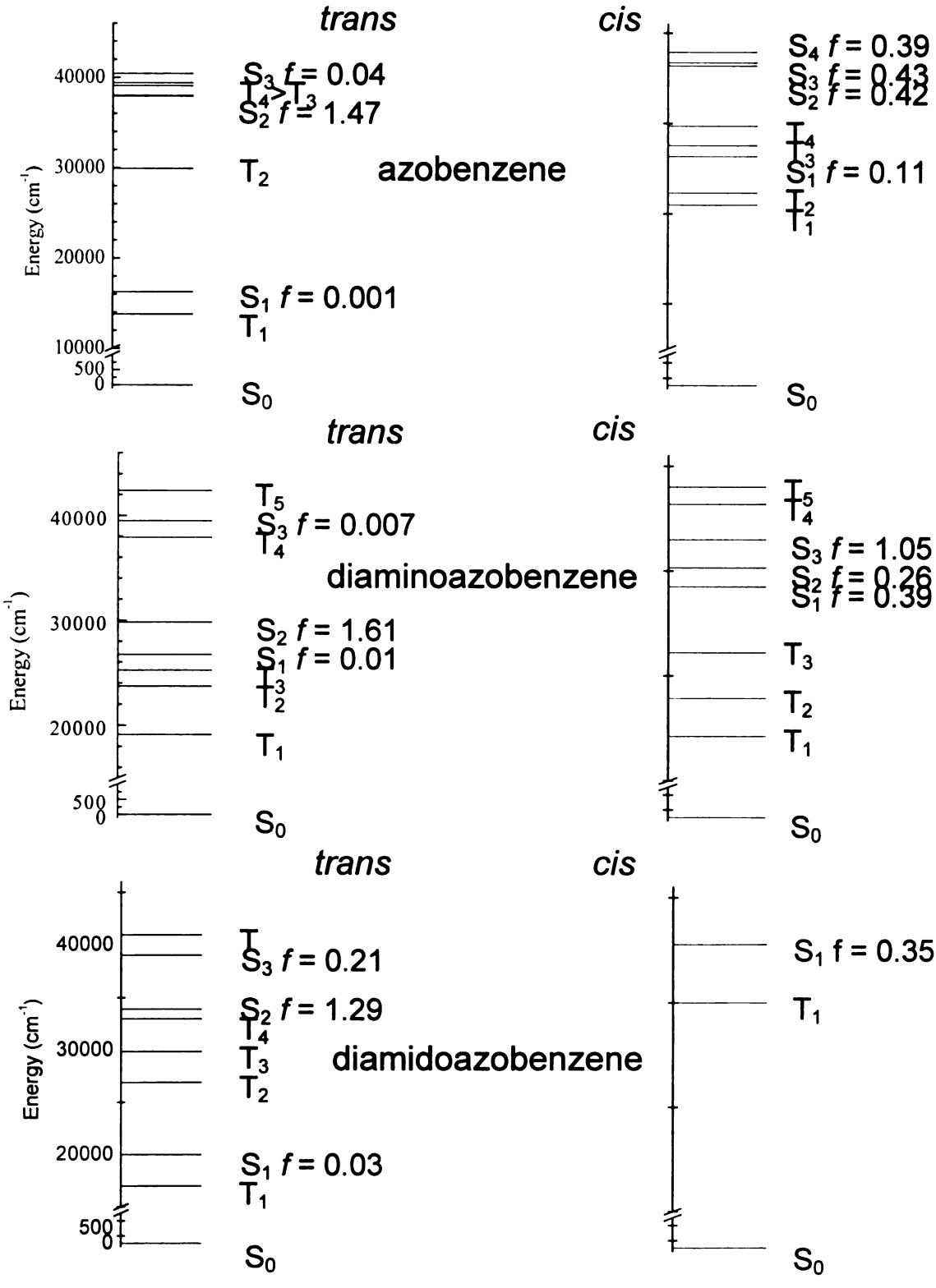


Figure 12: Calculated energy levels and oscillator strengths for azobenzene, diaminoazobenzene, and diamidoazobenzene.

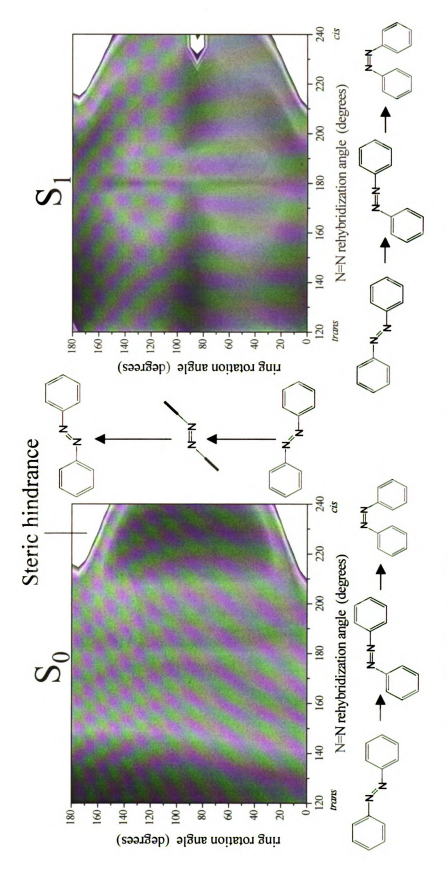


Figure 13: Calculated isomerization surfaces for inversion mechanism of azobenzene.

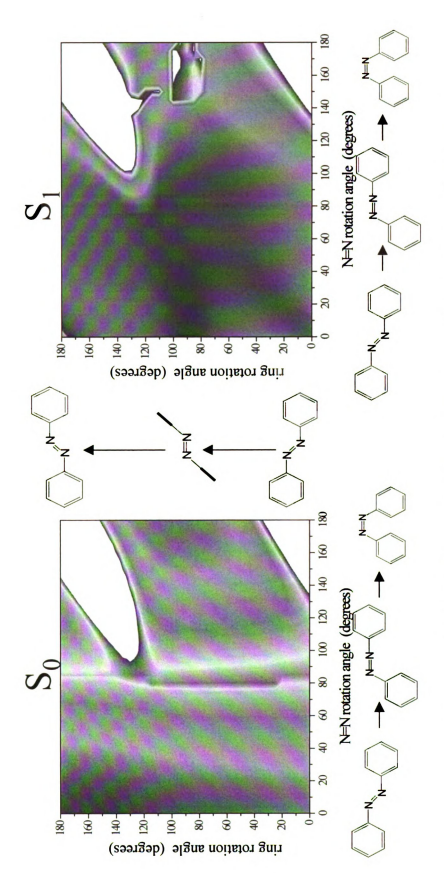


Figure 14: Calculated isomerization surfaces for rotation mechanism of azobenzene.

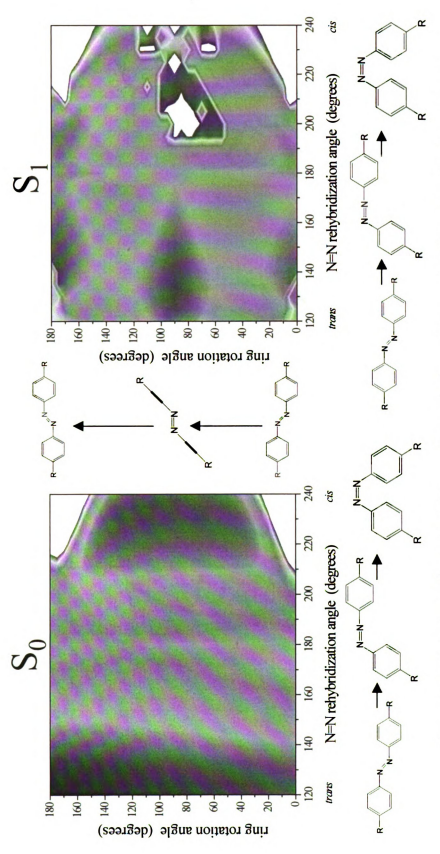


Figure 15: Calculated isomerization surfaces for inversion mechanism of p-diaminoazobenzene.

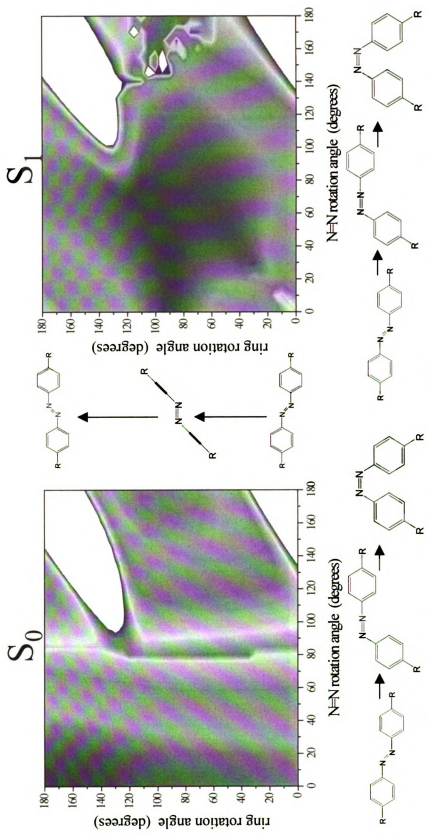


Figure 16: Calculated isomerization surfaces for rotation mechanism of p-diaminoazobenzene.

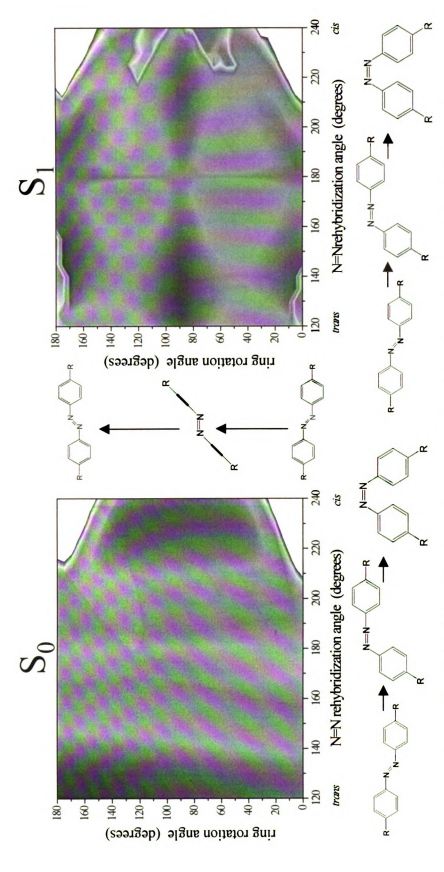


Figure 17: Calculated isomerization surfaces for inversion mechanism of p-diaminoazobenzene.

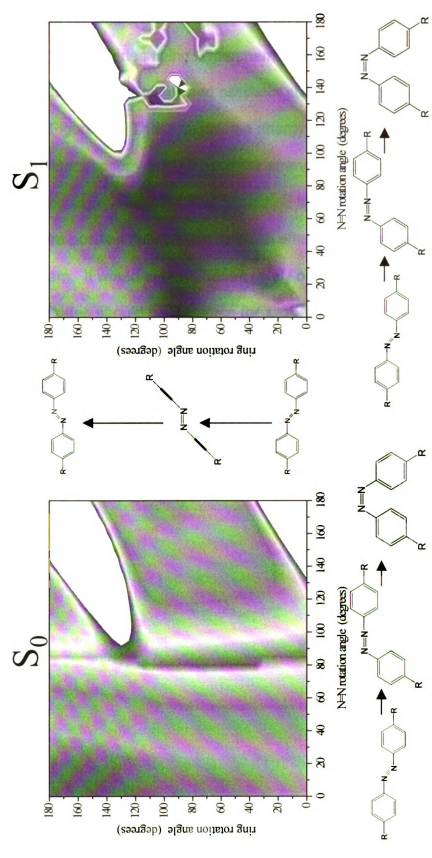


Figure 18: Calculated isomerization surfaces for rotation mechanism of p-diamidoazobenzene.

Semi-empirical calculations were conducted on the model series of *p*-disubstituted azobenzenes using Hyperchem® v. 6.0 and Microsoft Excel®. From these calculations energy levels and oscillator strengths can be calculated as presented in Figure 12. These calculated energy levels qualitatively agree with steady state spectroscopy but the oscillator strengths appear to deviate from those observed experimentally. The calculated isomerization surfaces suggest that at the *para* position substitution has little effect on the isomerization barrier and mechanism. It would appear, based solely on these calculations, that the isomerization rates should be the same for azobenzene, *p*-diaminoazobenzene, and *p*-diamidoazobenzene. We find these calculated results to be at odds with the experimental data, and take this finding to underscore the limitations inherent to parameterized calculations.

Literature Cited

- 1. Dewar, M. J. S.; Thiel, W. J. Am. Chem. Soc., 1977, 99, 4899.
- 2. Dewar, M. J. S.; Theil, W. J. Am. Chem. Soc., 1977, 99, 4907.
- 3. Fujino, T.; Arzhantsev, S. Y.; Tahara, T. J. Phys. Chem. A, 2001, 105, 8123.
- 4. Saito, T.; Kobayashi, T. J. Phys. Chem. A, 2002, 106, 9436.
- 5. Astrand, P.-O.; Ramanujam, P. S.; Hvilsted, S.; Bak, K. L.; Suauer, S. P. A. *J. Am. Chem. Soc.*, **2000**, *122*, 3482.
- 6. Ishikawa, T.; Noro, T.; Shoda, T. J. Chem. Phys., 2001, 115, 7503.
- 7. Fliegl, H.; Kohn, A.; Hattig, C.; Ahlrichs, R. J. Am. Chem. Soc., 2003, 125, 9821.
- 8. Zimmerman, G.; Chow, L. Y.; Paik, U. J. J. Am. Chem. Soc., 1958, 80, 3528.
- 9. Shultz, T.; Quenneville, J.; Levine, B.; Toniolo, A.; Martinez, T. J.; Lochbrunner, S.; Schmitt, M.; Shaffer, J. P.; Zgierski, M. Z.; Stolow, A. J. Am. Chem. Soc., 2003, 125, 8098.

Chapter 3

TIME RESOLVED SPECTROSCOPY

While steady state spectroscopy is useful for molecular analysis and identification, it does not provide direct information on molecular motion or isomerization for labile systems. We have used pump-probe transient absorbance spectroscopy and time correlated UV/Visible spectroscopy to investigate the isomerization process and the effects of substitution. The transient absorbance gives an insight into the interactions of photons with azobenzenes while time correlated UV/Visible absorption spectroscopy can yield time constants for the ground state back isomerization process.

Pump-probe spectroscopy utilizes two tuned laser beams to excite and monitor a molecular system. Chromophore concentration was kept low enough that the probability of dimer formation was not a major concern (10⁻³ M in 1-Octanol). This particular experiment can give insight into the overall excitation and relaxation processes of the system of interest. The technique selected for this investigation was transient absorbance. In such an experiment the magnitude, time scale, and sign of the signal all yield information. Figure 19 demonstrates that a positive-going signal is indicative of a bleaching experiment where the second photon measures absorption depletion induced by the first photon. A negative going signal is indicative of an induced absorption, where an electron is promoted from the first excited singlet state to a higher excited electron singlet state.

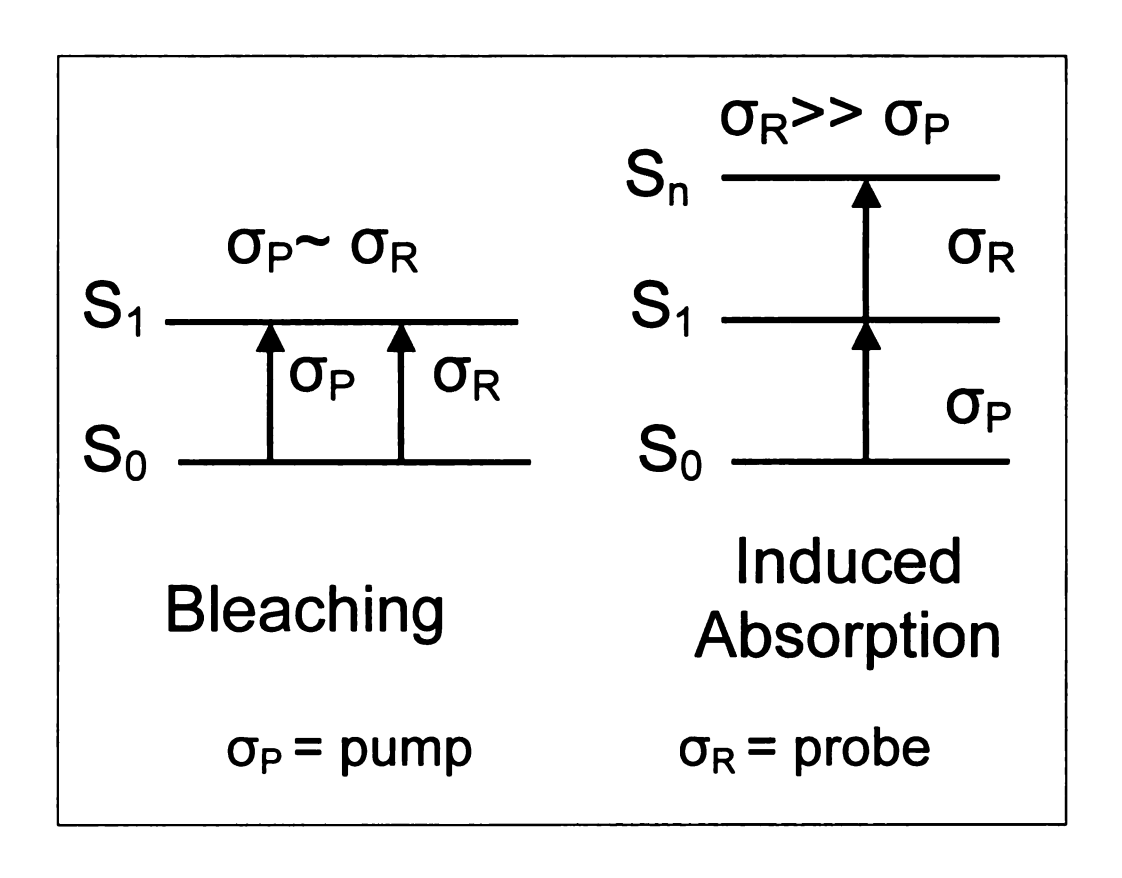


Figure 19 : Possible experiments available in a transient absorbance experiment.

The picosecond pump-probe laser spectrometer used in this experiment has been described in detail elsewhere, 1 and we provide only a brief synopsis of the system here. A mode-locked CW Nd:YAG laser (Coherent Antares 76-S) produces 30 W of average power (1064 nm, 100 ps pulses, 76 MHz repetition rate). The output of this laser is frequency-tripled to produce ~1.1 W average power at 355 nm with nominally the same pulse characteristics. The third harmonic light is used to excite two cavity-dumped dye lasers (Coherent 701-3) synchronously, with the output of both lasers being ~ 60 mW average power at 8 MHz repetition rate, producing 7 ps fwhm autocorrelation traces using a three plate birefringent filter. The pump and probe dye lasers are operated with Stilbene 420 dye (Exciton), at 435 nm and 445 nm, respectively. These wavelengths were selected to access the $S_1 \leftarrow S_0$ transitions of the azobenzenes. Encoding of the transient signals was accomplished using radio- and audiofrequency triple modulation, with synchronous demodulation detection.²⁻⁴ Samples for the transient absorbance experiments were prepared by dissolving the azobenzene derivative of interest in 1-octanol to achieve a 1x10⁻⁴ M concentration.

We have measured the transient optical response of the several disubstituted azobenzenes. For all of the measurements we report here, we have excited the compound at 445 nm and interrogated the result of that excitation at 435 nm. These wavelengths access the lowest allowed singlet transition in each compound. Azobenzene produces a transient response different from that of the substituted species. Specifically, we observe an

induced absorption centered at zero delay time, with no resolvable longer time components. This feature is independent of solvent identity and it possesses a unique characteristic; the transient response exhibits a time profile that is reproducibly narrower than the instrument response function (Figure 20a). This anomalous behavior results from the transient signal being a multiphoton process. The instrument response function is linear in the intensity of each incident beam, and for the experimental signal to be shorter in time than the instrument response, it must depend on the intensity of the incident beam(s) in a manner different than that of the response function; i.e. the signal must scale with more than two photons overall. The negative sign of the experimental signal indicates that it results from an induced absorption, and given the low intensity of the probe beam, it is most likely that the pump beam undergoes resonanceenhanced two photon absorption, with the probe sensing induced absorption from the final state of the two photon transition to a higher excited singlet state. Given the low intensity of the probe relative to the pump, the probability of the nonlinear response being dominated by the probe is negligible, even though it is at essentially the same wavelength as the pump. This is the simplest explanation consistent with both the anomalous temporal width and the sign of the transient response, and we note that this sequence of events involves at least 8.43 eV of photon energy, slightly less than the ionization threshold of

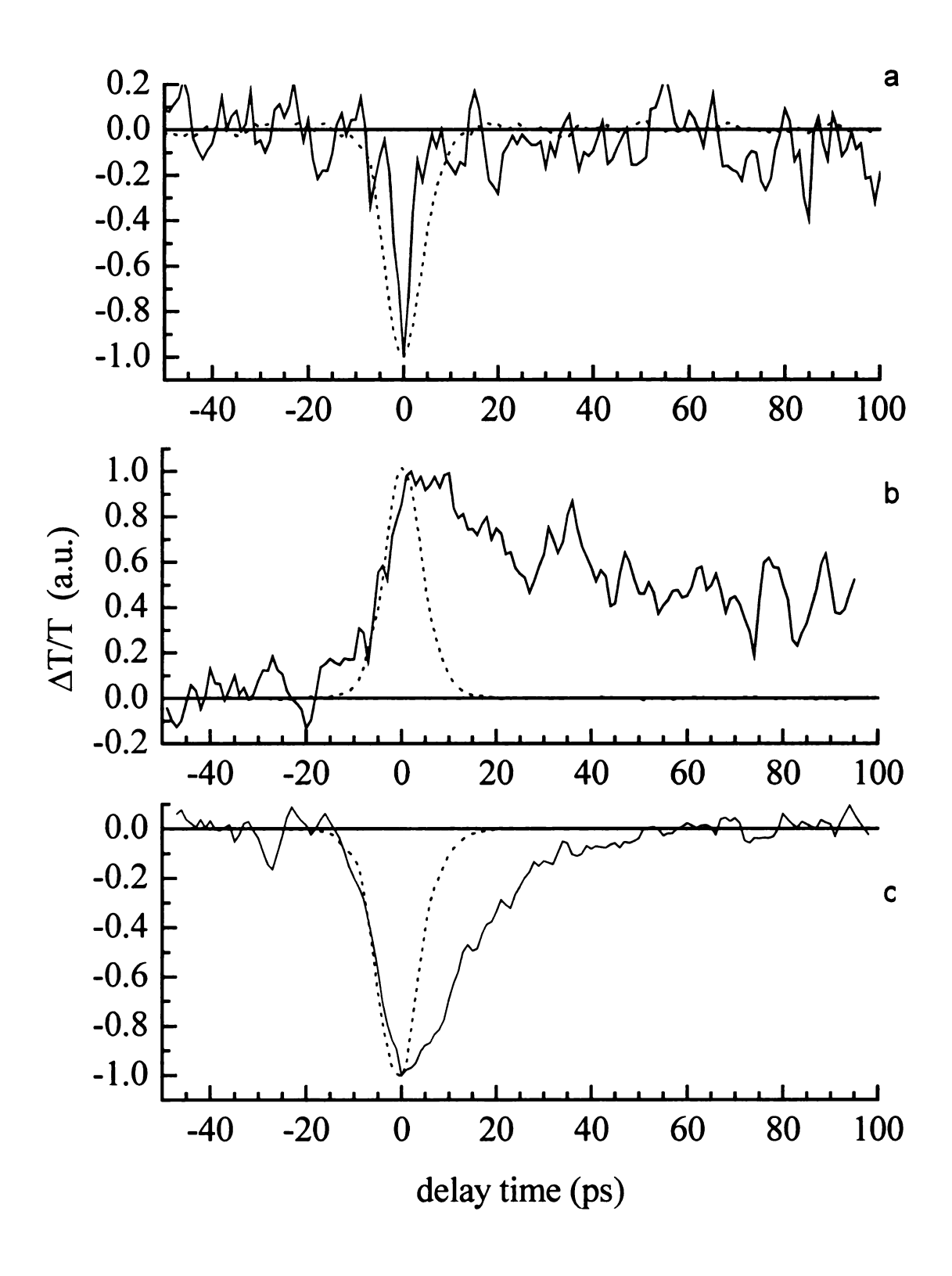


Figure 20 : Transient absorbance response of a) azobenzene b) p-diaminoazobenzene c) p-diamidoazobenzene.

azobenzene.⁵ Understanding the details of this multiphoton process will clearly require further investigation. Because of the small signal intensities, we were not able to acquire the intensity-dependence of this transient response. Given the uncertainty in the number of photons involved in this process, accurate assignment of the states involved is not feasible.

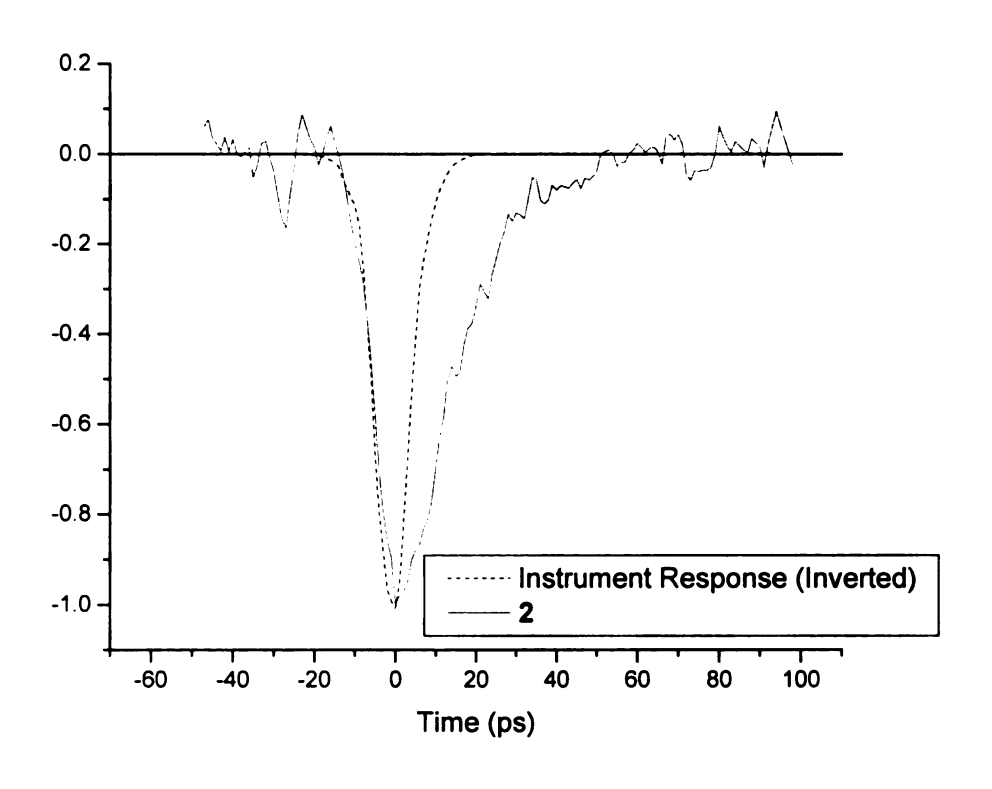
The transient response of p-diaminoazobenzene differs substantially from both azobenzene and p-diamidoazobenzene. We observe for the diamino compound a positive (bleaching) transient signal with a 116 ps single exponential decay time constant (Figure 20b, Table 3). The time constant is not sensitive to the identity of the solvent in which p-diaminoazobenzene is dissolved, and its functionality implies that excitation at ~440 nm is to the lowest lying excited singlet state. Calculations (Figure 12) suggest that the dominant transition for the trans conformer of this compound is the $S_2 \leftarrow S_0$ transition, with the $S_1 \leftarrow S_0$ transition being characterized by a vanishingly small oscillator strength. The decay time constant seen for the transient data suggest that we are accessing the $S_1 \leftarrow S_0$ transition, and the steady state data show the oscillator strength for this transition to be significant. In contrast to the results for azobenzene, the positive transient signal implies that excited state absorption $(S_n \leftarrow S_1)$ is inefficient for p-diaminoazobenzene at \sim 440 nm, and the observed transient is simply a ground state recovery response.

Compound	Decay functionality	Time constant
		(ps)
Azobenzene	induced absorption	< IRFª
p-	bleaching	116 ± 12
diaminoazobenzene	bleaching	110112
1	induced absorption	13 ± 3
2	induced absorption	14 ± 1
3	induced absorption	16 ± 1
4	induced absorption	16 ± 1
5	induced absorption	15 ± 1

Table 3. Transient optical decay functionalities and time constants of azobenzene, *p*-diaminoazobenzene and the *p*-diamidoazobenzenes **1-5**.

^a IRF = instrument response function, 10 ps fwhm.

The diamidoazobenzenes exhibit a transient response that is independent of length of the amido aliphatic chain. For all measurements we recover an induced absorption signal, with a characteristic time constant of ~ 15 ps, measurably longer than the instrument response function, in contrast to that seen for azobenzene (Figure 21, Table 3). The induced absorption is likely the result of $S_n \leftarrow S_1$ absorption of the probe pulse following population of the S_1 state by the pump pulse. In this model, the time constant of ~15 ps is determined by the lifetime of the S_1 state. For azobenzene, a ~15 ps transient has been seen previously.^{6,7} We do not observe such a decay for azobenzene in this work because we are not pumping the $S_2 \leftarrow S_0$ transition for the *trans* form. The origin of the 15 ps transient in azobenzene was ascribed to a "bottleneck" state on the S₂ isomerization surface. It is unlikely that the diamidoazobenzene ~15 ps recovery time is analogous to that seen for azobenzene (we are not exciting the $S_2 \leftarrow S_0$ transition of diamidoazobenzene), although it is possible that a "bottleneck" could be present on the S₁ isomerization surface of diamidoazobenzenes. Clearly, more investigation is required to assign the origin of this transient. As with the calculations for p-diaminoazobenzene, we find that the p-diamidoazobenzenes are characterized by a low lying first excited singlet state, and the $S_1 \leftarrow S_0$ transition is calculated to have a small oscillator strength. This theoretical result appears to be at odds with the experimental steady state and transient optical responses.



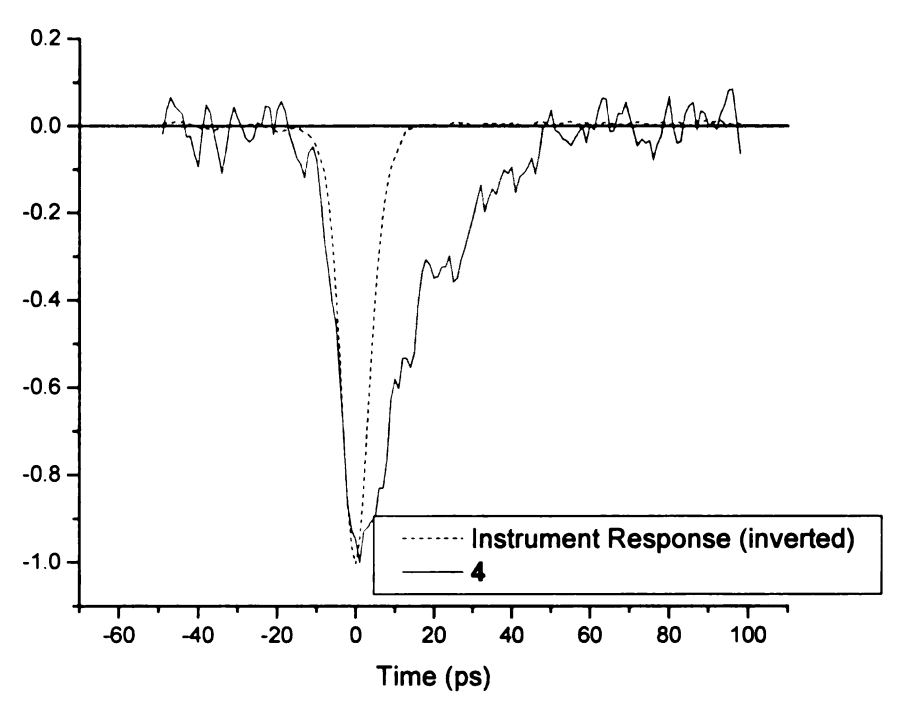


Figure 21 : Transient absorbance response of two p-diamidoazobenzenes.

The azobenzene derivatives we study here exhibit remarkable substituent-dependent variation in their steady state and time-resolved optical responses, and these findings are mirrored by substantial changes in the electronic state energies and singlet transition oscillator strengths calculated at the semi-empirical level. It appears, based on a comparison of experimental and calculated results for these compounds, that the transition energies are predicted relatively well, but the oscillator strengths for these transitions are not. Given these findings, intuition may suggest that the isomerization behavior of these molecules would likewise vary with substitution, and we examine this issue next.

To understand the isomerization behavior of azobenzene and the symmetrically disubstituted azobenzenes, we have evaluated the branching ratio for isomer formation and the recovery time required for the samples to return to an equilibrium ground state population distribution. The branching ratio data is indicative of the location of the ground state surface maximum and the excited electronic state surface minimum. In the limit that these two electronic state features exist at the same point in conformational space, we would expect a branching ratio of 1 (*i.e.* 50% of the excited molecules relax to form a *trans* conformer and 50% relax to form a *cis* conformer. Deviations from this ideal behavior are indicative of either a non-correspondence between the electronic state surface minima and maxima or a ground state potential energy surface that is not well characterized in the context of Rulliere's model.⁸

If the azobenzene sample begins as a ratio near 50% of either isomer upon irradiation this ratio can be shifted to promote one isomer over the other.

This can be seen in Figure 22 where **5** is promoted to primarily the *cis* form upon 90 minutes of irradiation under an ultraviolet lamp. These spectra were taken in 1-octanol on the spectrometer previously mentioned. Upon varying reaction conditions and evaluating nearly no spectral alteration it was determined that the instrument could be affecting the experiment. The spectrometer used was a dual beam instrument where the sample beam constantly illuminates the sample. This was found to be a problem for both the branching ratio and the time correlated relaxation experiment. To counteract this problem the instrument was modified by placing a neutral density filter in the path in front of the sample holder as pictured in Figure 23.

To make a meaningful analysis of the branching ratio it is necessary to quantitatively analyze the steady state peaks corresponding to both *cis* and *trans* isomers. Concentrations work well for this application where each peak gives the concentration of that isomer. In the case of azobenzene the peak at 318 nm can be used to calculate the concentration of *trans* azobenzene at that moment. Likewise the peak at 254 nm can be used to calculate the concentration of *cis* azobenzene at that moment. The branching ratio can then be obtained by evaluating the ratio of one of the concentrations versus the total concentration of isomers. To calculate the concentration of each peak the molar extinction coefficient was needed at any wavelength that proved to identify an isomer. The molar extinction coefficients were calculated by evaluating the change in absorbance for a dilution series of the compounds in methanol. These yielded graphs as in Figure 24 where the slope is the extinction coefficient and the line

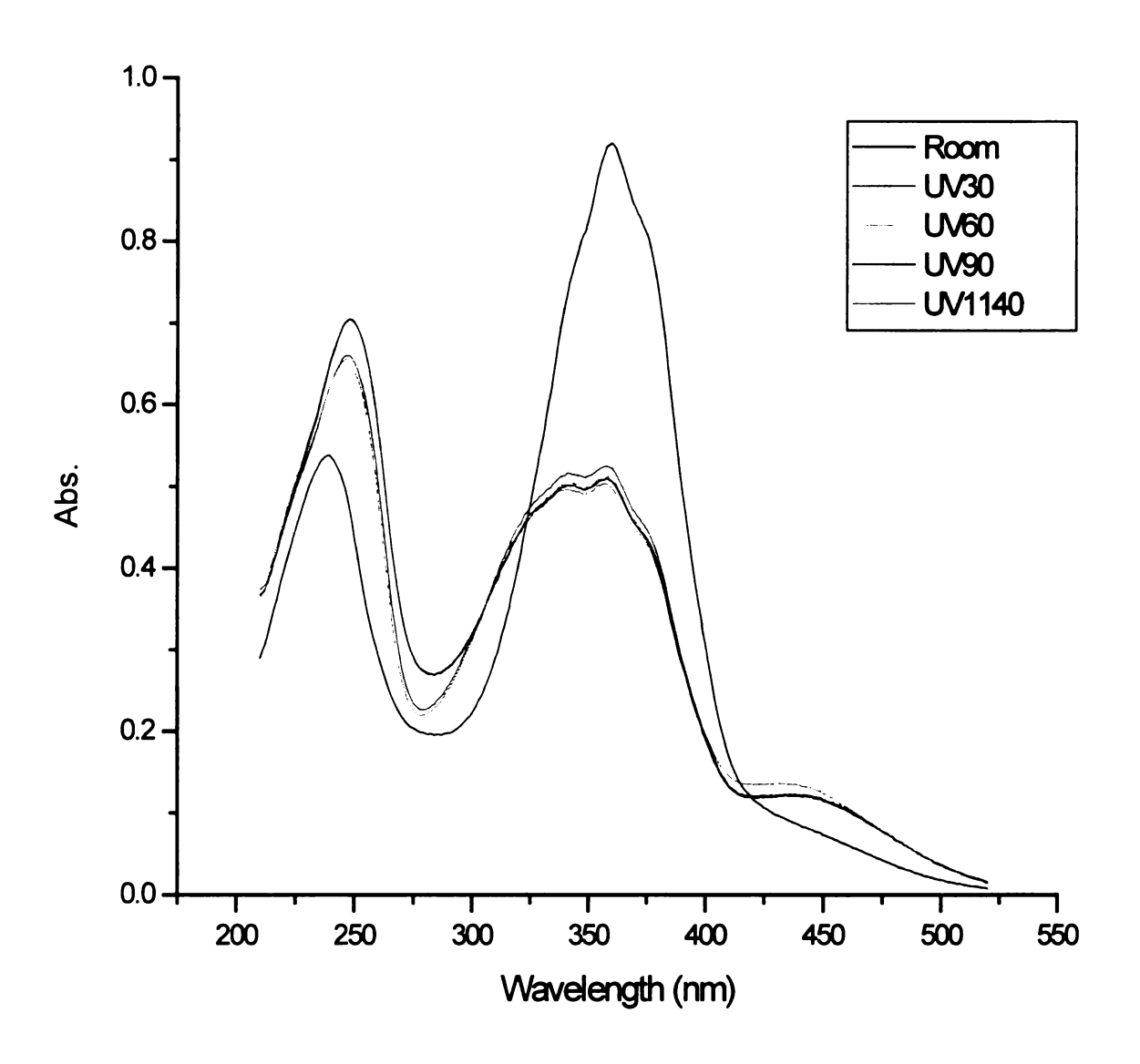


Figure 22 : Absorbance spectra of **5** upon varying durations of ultraviolet irradiation.

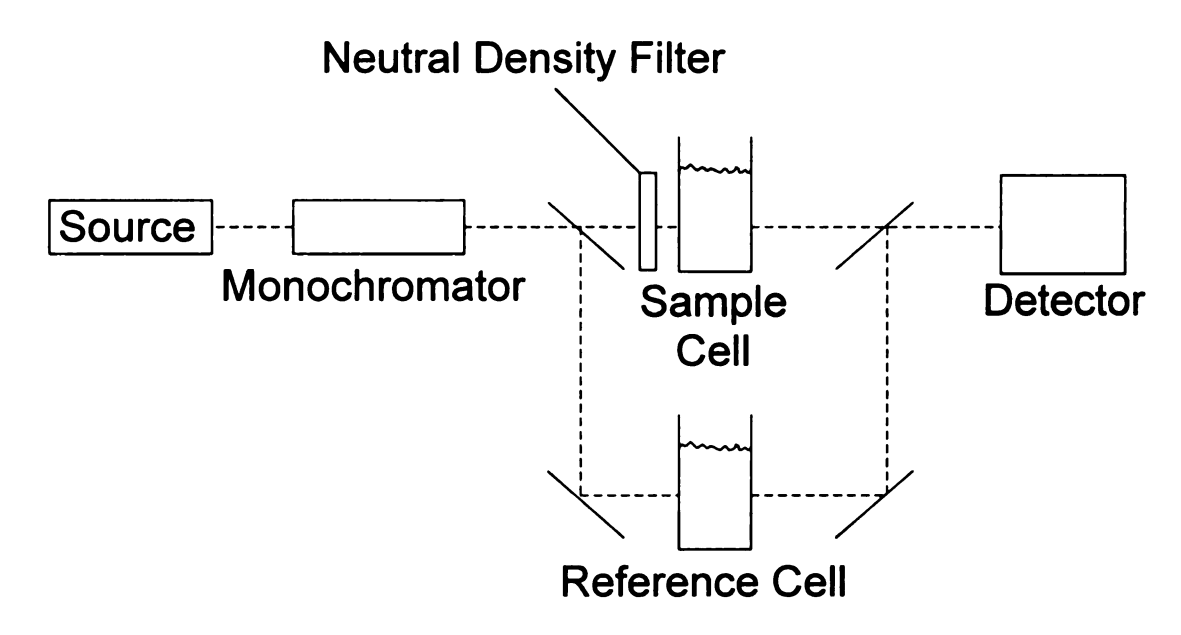


Figure 23 : Block diagram of UV/Vis instrument

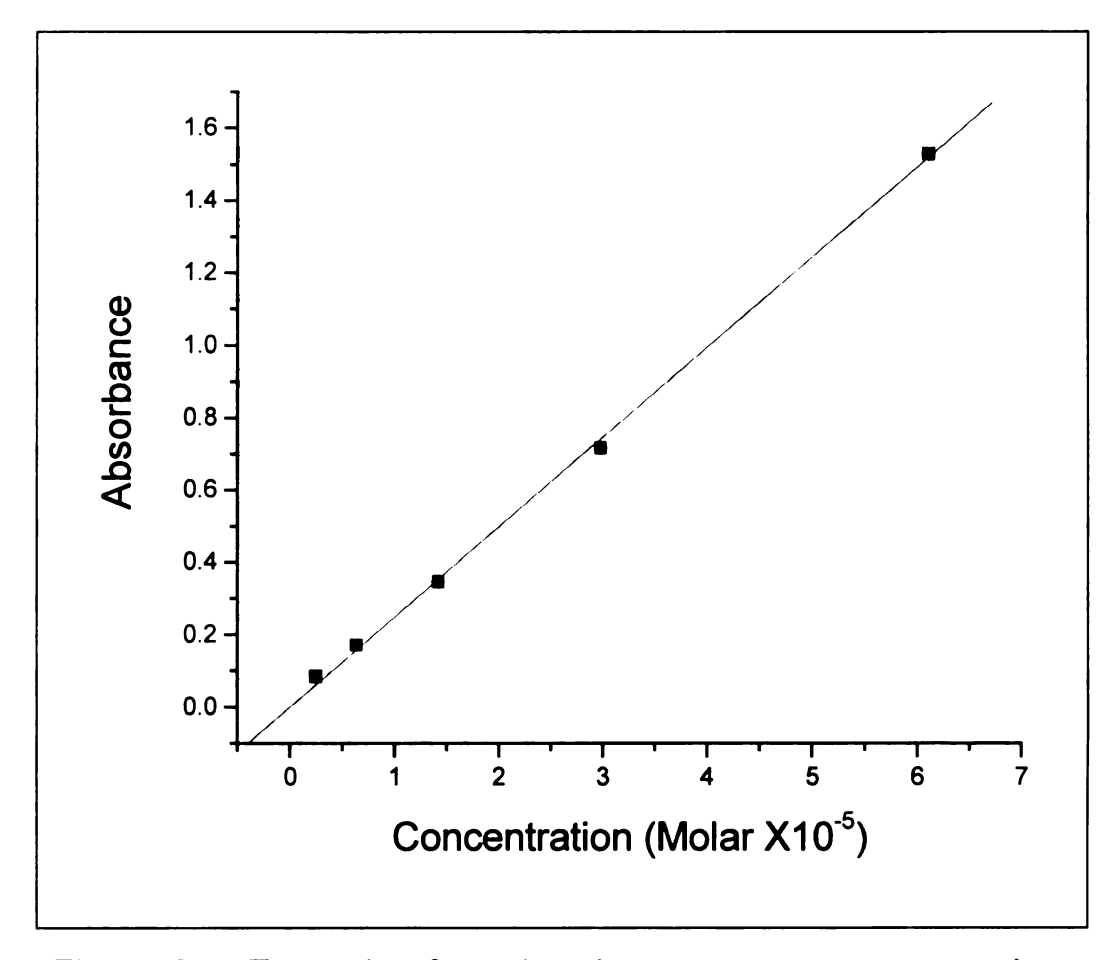


Figure 24: Example of an absorbance versus concentration graph used to determine molar absorptivity.

should go through the origin since at zero concentration there should be no absorbance. Subtracting the x-intercept from the concentration and then reevaluating the absorbance versus concentration graph can correct any deviation from the origin observed. Methanol was used as the solvent due to the high degree of solubility of all the molecules of interest. Solvent selection was not crucial since the molar extinction coefficient is essentially solvent independent. The coefficients along with the corresponding wavelengths are presented in Table 2.

To characterize the branching ratio, we irradiate a sample until the ratio of *trans* to *cis* remains constant, as measured by absorption spectroscopy.

Because the extinction coefficients of the *cis* and *trans* bands will, in general, differ, we need to correct the data either through band ratio measurements or by direct conversion of the absorbance data to concentration data using Beer's law. Upon UV irradiation, the ratio of *trans* to *cis* conformers reaches a steady state, which recovers to the equilibrium ratio once UV irradiation of the sample is stopped. The steady state [*trans*]/[*cis*] ratio, prior to recovery, is 0.19 for azobenzene, 0.51 for diamidoazobenzene and 4.5 for diaminoazobenzene. We note the similarity of azobenzene and diamidoazobenzene, and the contrasting behavior or diaminoazobenzene. These data point to the barrier height for *cis* → *trans* isomerization being largest for azobenzene and smallest for *p*-diaminoazobenzene, in agreement with the direct measurements we report below.

Of perhaps greater significance than the branching ratio data are those for the isomerization recovery. We have measured the isomerization recovery time constants for azobenzene, p-diaminoazobenzene and p-diamidoazobenzene. The time constants are for $cis \rightarrow trans$ conversion and vary enormously with substitution and scale qualitatively with the energy of the dominant electronic transition of the chromophores. For azobenzene, we find that the recovery time after photoisomerization is 10,900 minutes (Figure 25), for the pdiamidoazobenzenes, the recovery time is 317 minutes (Figure 26), and for pdiaminoazobenzene, the recovery time is 4.7 minutes (Figure 27). These remarkably different time constants for trans recovery are due to variations in the isomerization barrier height, which are related electron density distribution about the azo bonds in these compounds. While the back isomerization time constants are remarkably different for these compounds, it is important to keep in mind that there is a logarithmic relationship between the measured time constant and the barrier height. Since the process of interest is a monomolecular we have used the Arrhenius equation to calculate isomerization barrier heights. Where A is a

$$k = \frac{1}{\tau} = Ae^{\frac{-\Delta E}{kT}}$$

prefactor, τ is measured from experimental data, and ΔE is the variable of interest. We have calculated the barrier heights consistent with the experimental back-isomerization data for the substituted azobenzenes, assuming a prefactor for the activated process of 10^{13} Hz. For *p*-diaminoazobenzene, with a characteristic recovery time constant of 2.4 minutes, we calculate a barrier height of 20.8 kcal/mol, for *p*-diamidoazobenzene, with a recovery time constant of 317

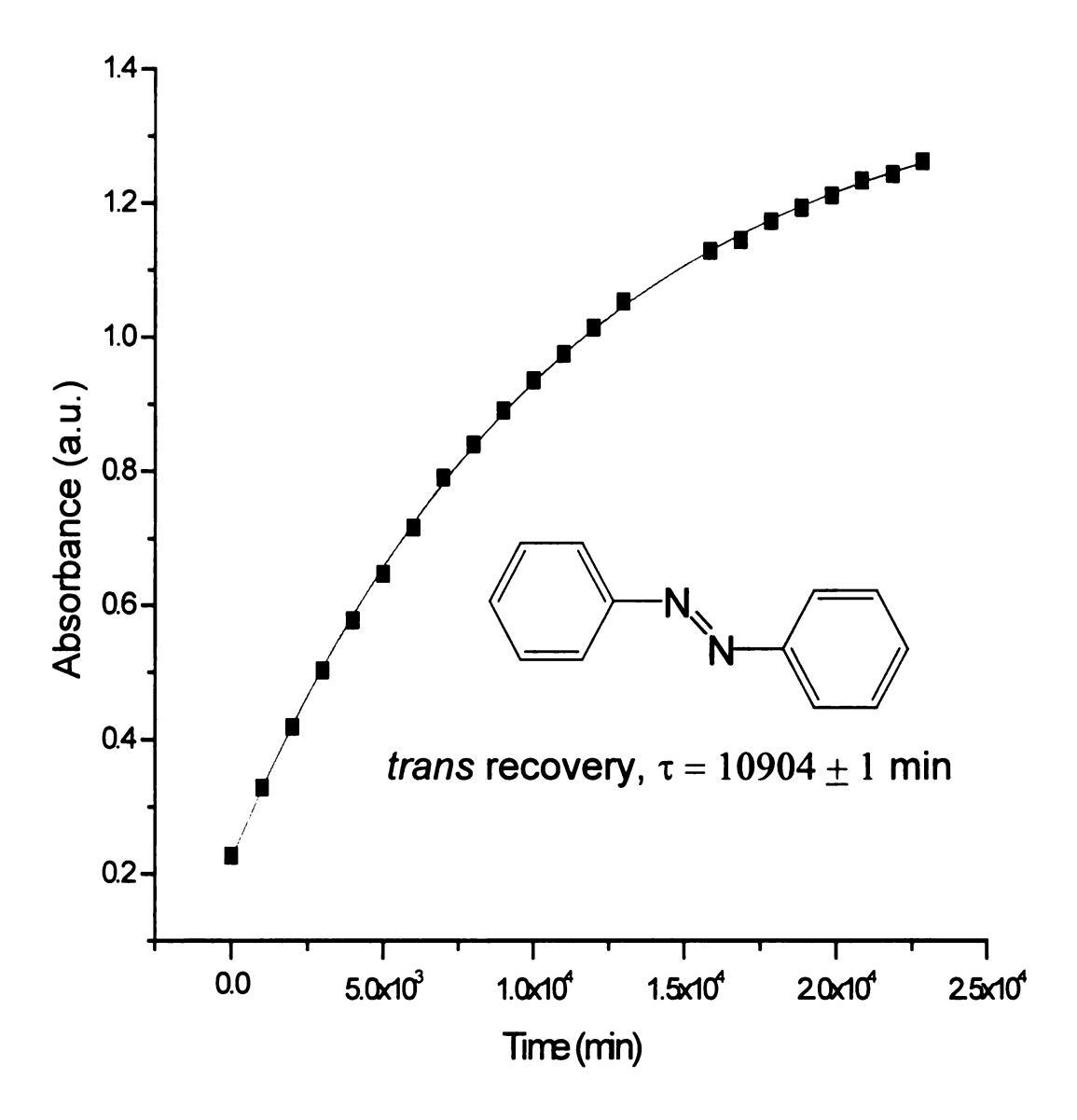


Figure 25: Recovery of the absorption due to the *trans* band in azobenzene at 318 nm.

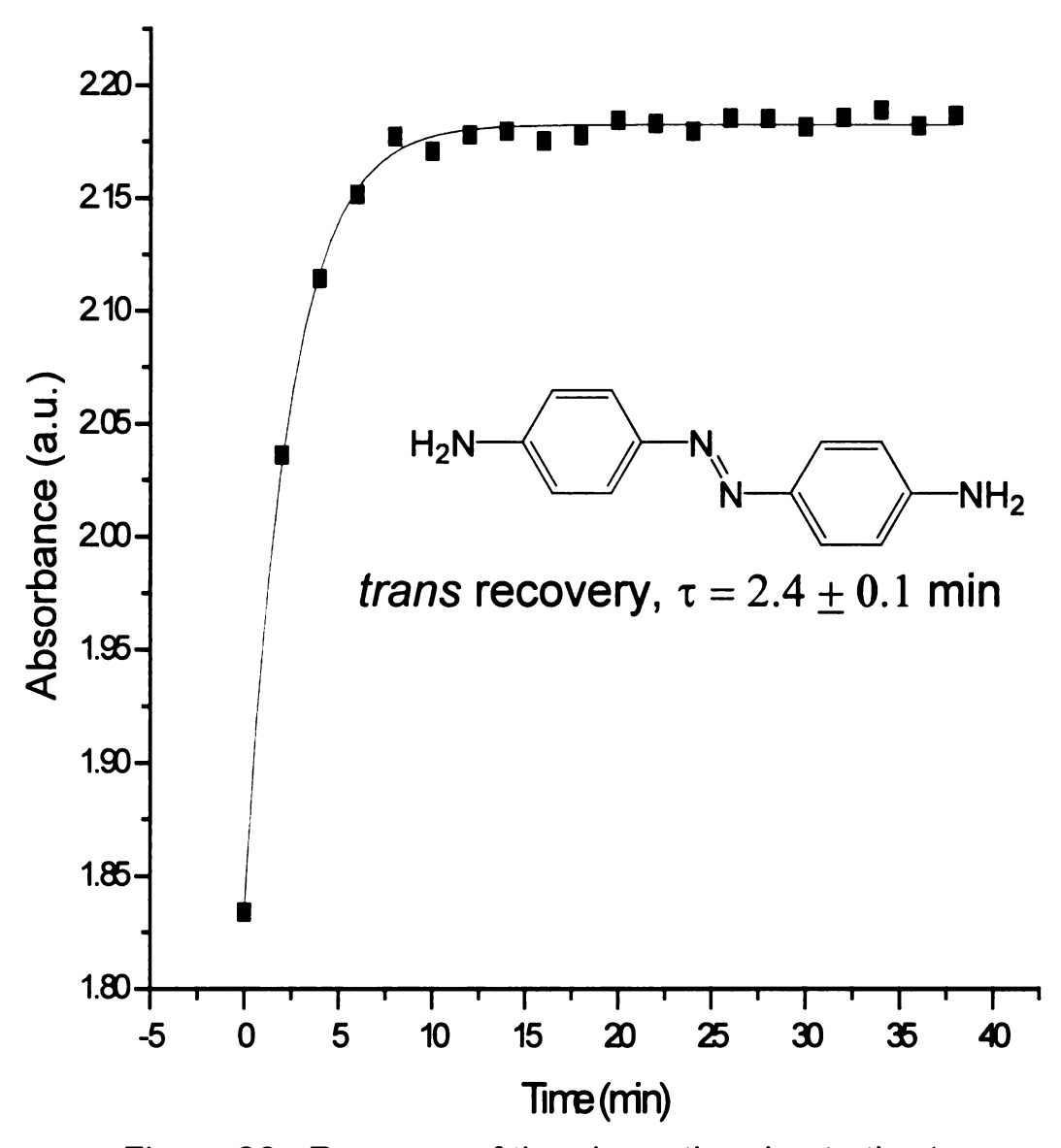


Figure 26 : Recovery of the absorption due to the *trans* band in *p*-diaminoazobenzene at 370 nm.

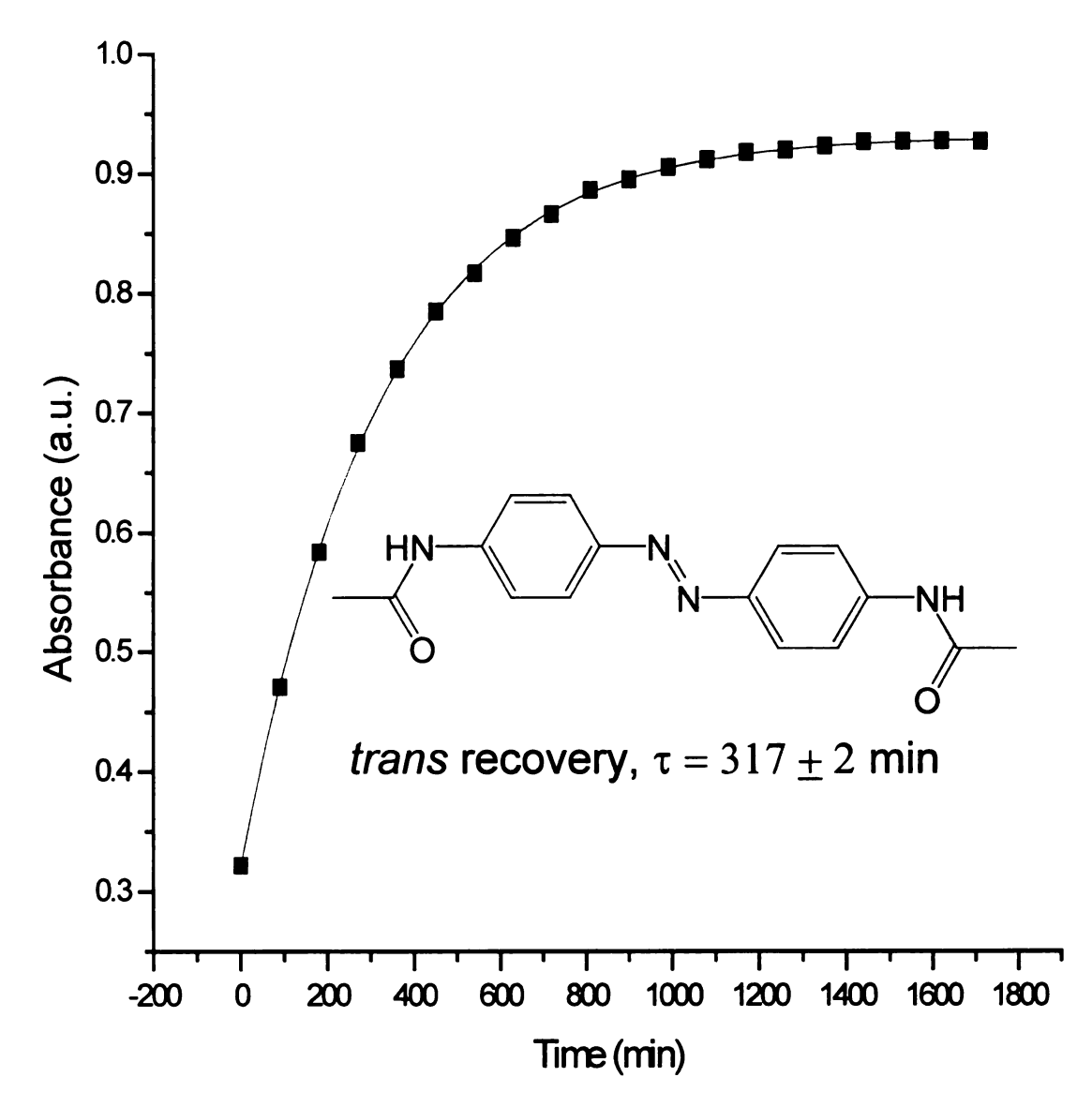


Figure 27 : Recovery of the absorption due to the trans band in p-diamidoazobenzene at 370 nm.

minutes, we calculate a barrier height of 23.7 kcal/mol and for azobenzene, with a recovery time constant of 10,900 minutes, we calculate a barrier height of 25.8 kcal/mol. These barrier heights, for S_0 $cis \rightarrow trans$ conversion vary substantially less than the recovery time data would seem to imply, owing to the logarithmic relationship between the recovery rate constant and the barrier height. The semi-empirical calculations for azobenzene are in qualitative agreement with the experimental data.

We note that there is an inverse correlation between barrier height and electron donor strength of the para substituents. This correlation is the result of an effective increase in the average electron density of the π^* (antibonding) state, reducing the effective bond order of the N=N bond and thereby reducing the isomerization barrier height. We seek to understand the detailed basis for this relationship and find that the linear optical response of these compounds is useful for this purpose. The ground state (thermal) barrier for isomerization is correlated inversely with the transition cross section of the first allowed electronic transition for these azobenzenes. All of the azobenzenes studied here have transitions in the 400 - 450 nm region (Figure 11), so it is not the *energy* of the S_1 ← S₀ transition that is related to the thermal back isomerization barrier height. Rather, it is the transition cross section of the lowest energy transition that is related to the barrier height. We rationalize this relationship by noting that a large transition cross section is reflective of large overlap integrals for the transitions. The isomerization barrier height is related to the bond order of the N=N bond, and the $S_1 \leftarrow S_0$ transition coordinate is thought to lie along the long

axis of the azobenzene molecule. We postulate that the isomerization and electronic transition coordinates are nearly the same. The ground electronic states (HOMOs) of the azobenzenes are characterized by a relatively high bond order of \sim 2 for the N=N bond. The first excited singlet states (HOMOs) of these compounds are characterized by a substantial reduction in electron density and thus bond order on excitation. Because the activation barrier for ground state back isomerization of the azobenzenes involves a high energy intermediate state, mixing with states in the S_1 manifold is possible, and the strength of this coupling is reflected in the transition cross sections of the $S_1 \leftarrow S_0$ transitions for both the cis and trans forms. Thus, the larger the transition cross section for the $S_1 \leftarrow S_0$ transition (Table 2), the more single-bond character there will be for the transition state on the S_0 isomerization surface, giving rise to a lower barrier height. This explanation provides qualitative agreement with the experimental data and does not invoke coupling of higher excited electronic states.

It was determined through both time resolved experiments that the identity of the para substituent alters the overall time of isomerization. It was also seen that the *p*-diaminoazobenzene seems to be different than the other *p*-disubstituted azobenzenes. This result can be seen in Table 3 and Figures 29 to 31.

Literature Cited

- 1. Jiang, Y.; Hambir, S. A.; Blanchard, G. J. Opt. Commun., 1993, 99, 216.
- 2. Bado, P.; Wilson, S. B.; Wilson, K. R. Rev. Sci. Instrum., 1982, 53, 706.
- 3. Andor, L.; Lorincz, A.; Siemion, J.; Smith, D. D.; Rice, S. A. *Rev. Sci. Instrum.*, 1984, 55, 64.
- 4. Blanchard, G. J.; Wirth, M. J. Anal. Chem., 1986, 58, 532.
- 5. Shultz, T.; Quenneville, J.; Levine, B.; Toniolo, A.; Martinez, T. J.; Lochbrunner, S.; Schmitt, M.; Shaffer, J. P.; Zgierski, M. Z.; Stolow, A. *J. Am. Chem. Soc.*, **2003**, *125*, 8098.
- 6. Lednev, I. K.; Ye, T.-Q.; Matousek, P.; Towrie, M.; Foggi, P.; Neuwahl, F. V. R.; Umapathy, ,S.; Hester, R. E.; Moore, J. N. *Chem. Phys. Lett.*, **1998**, *290*, 68.
- 7. Lednev, I. K.; Ye, T.-Q.; Abbott, L. C.; Hester, R. E.; Moore, J. N. *J. Phys. Chem. A*, **1998**, *102*, 9161.
- 8. Rulliere, C. Chem. Phys. Lett., 1976, 43, 303.

Conclusion

The goal of this research was to evaluate azobenzene derivatives as possible probes and interlayer linkages in stacked polymer systems. The use of an isomerizable interlayer linkage enables the development of optical storage devices based on the change of conformation and polymers for separations based on change in free volume associated with isomerization. The isomerization and spectroscopy of azobenzene must fully be understood before any development can be achieved. Selection of the proper azobenzene to work with was determined by engineering necessities and ability to be synthesized. The steady state spectroscopy gave little insight into the mechanism and overall behavior of the isomerization process. To achieve this goal a series of calculations were performed on a series of p-disubstituted azobenzenes. These calculations suggested that the isomerization mechanism was independent of substitution in the para positions. To validate the calculations a series of time correlated spectroscopy techniques were performed. Pump-probe transient absorbance spectroscopy was used to determine the affects of photon absorption on the molecules. Time correlated UV/Visible spectroscopy was conducted to determine the time constant for isomerization. Upon analyzing the data it was determined that further calculations were needed to fully understand the results.

A series of *p*-diamidoazobenzenes was synthesized from *p*-diaminoazobenzene. The synthesis selected was based on a classic polyamido polymerization route using only monofucntional monomers to reach the desired

compounds. The yields obtained for each compound are presented in Table 1. Careful purification techniques greatly improved purity and only mildly affected yield. The UV/Vis spectrum shifted with substitution as suspected. All of the *p*-diamidoazobenzenes absorb at the same wavelength, which is shifted from pure azobenzene and *p*-diaminoazobenzene. The NMR spectroscopy showed the shifts expected and was used as a tool to analyze the purity of the synthesized compounds.

Semi-empirical calculations were performed on the series of azobenzenes synthesized, azobenzene, and the *p*-diaminoazobenzene. For these calculations the lowest energy conformer was determined by a PM3 basis set. Energy levels and oscillator strengths were calculated yielding Figure 12. From steady state and time-correlated spectroscopy it was determined that the energy levels were accurate but the oscillator strengths were incorrect. A set of isomerization surfaces was calculated for each one of the molecules based both on the inversion and rotation isomerization mechanisms. From these surfaces it was determined that substitution at the para position does not affect the isomerization mechanism.

From the transient absorbance experiment it was found that azobenzene experiences a multi-photon process upon photon absorption.

Diaminoazobenzene demonstrates a bleaching experiment, and diamidoazobenzene exhibits an induced absorption upon irradiation. This change in process upon irradiation is indicative of an electronic state alteration. This is understandable in that the conjugated pi system of the azobenzene

moiety is also in conjugation with either the amine or amide nitrogen depending on which species is being evaluated. It was found through time correlated UV/Vis spectroscopy that the substitution also affects the time constant of the isomerization process. This is at odds with the calculations performed. The explanation is that the alterations in time constant observed are actually due to very slight changes in energy level. The order of time constants is distributed as diamino, diamido, and then azobenzene having the longest time constant. These time constants are separated by an order of magnitude.

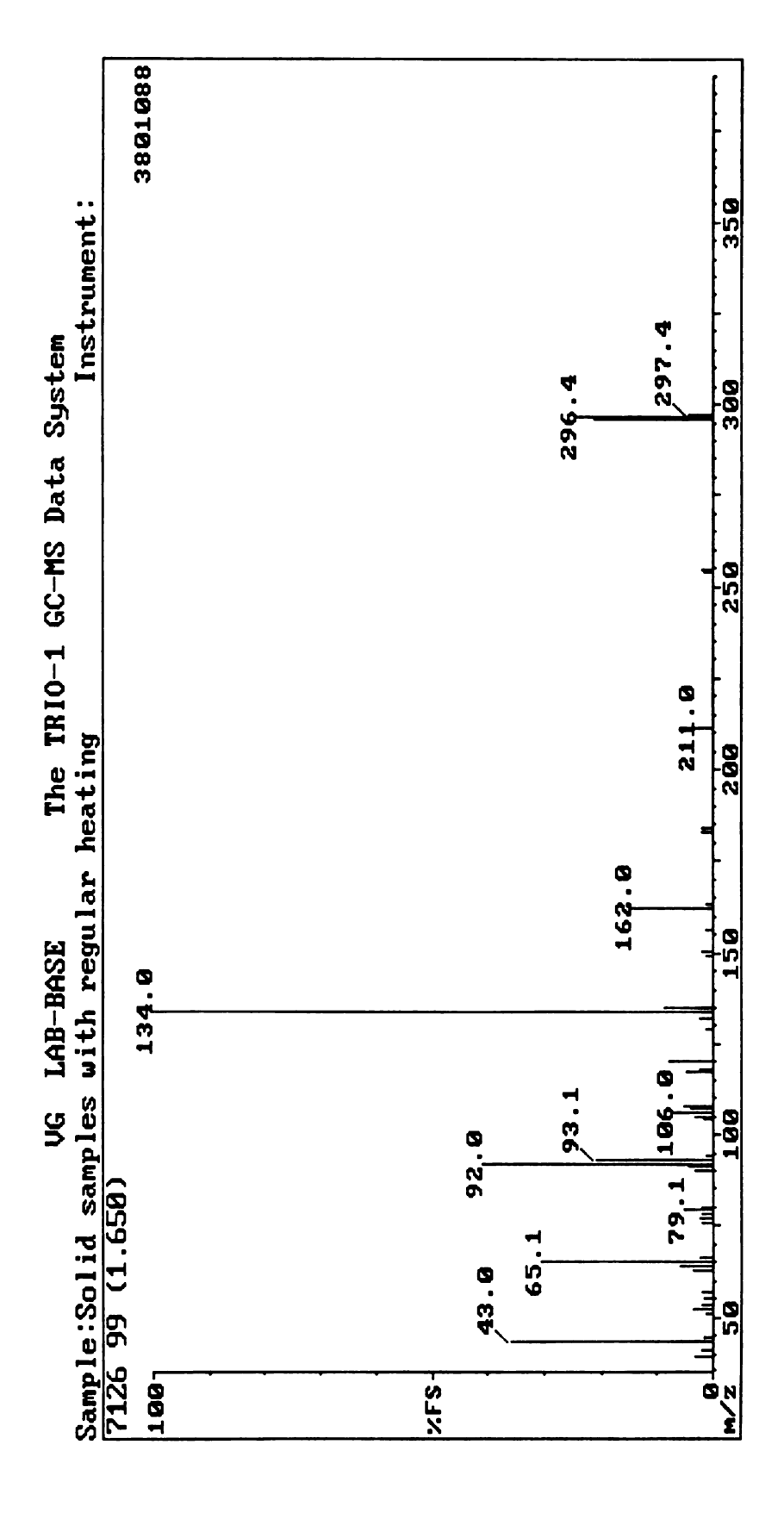
The future work on this project leads to the adoption of a different molecule for the probing and storage applications. This decision is based on the limited control on the isomerization process that a scientist has on the azobenzene moiety based solely on substitution. Two classes of molecules present possible routes of investigation, fulgides and spiropyrans. Azobenzene compounds still exhibit the wanted ability to drastically alter the free volume of a stacked polymer system upon isomerization. The next step in realizing the separation membrane is to functionalize the ends of the alkane chains on the diamidoazobenzene species.

APPENDICES

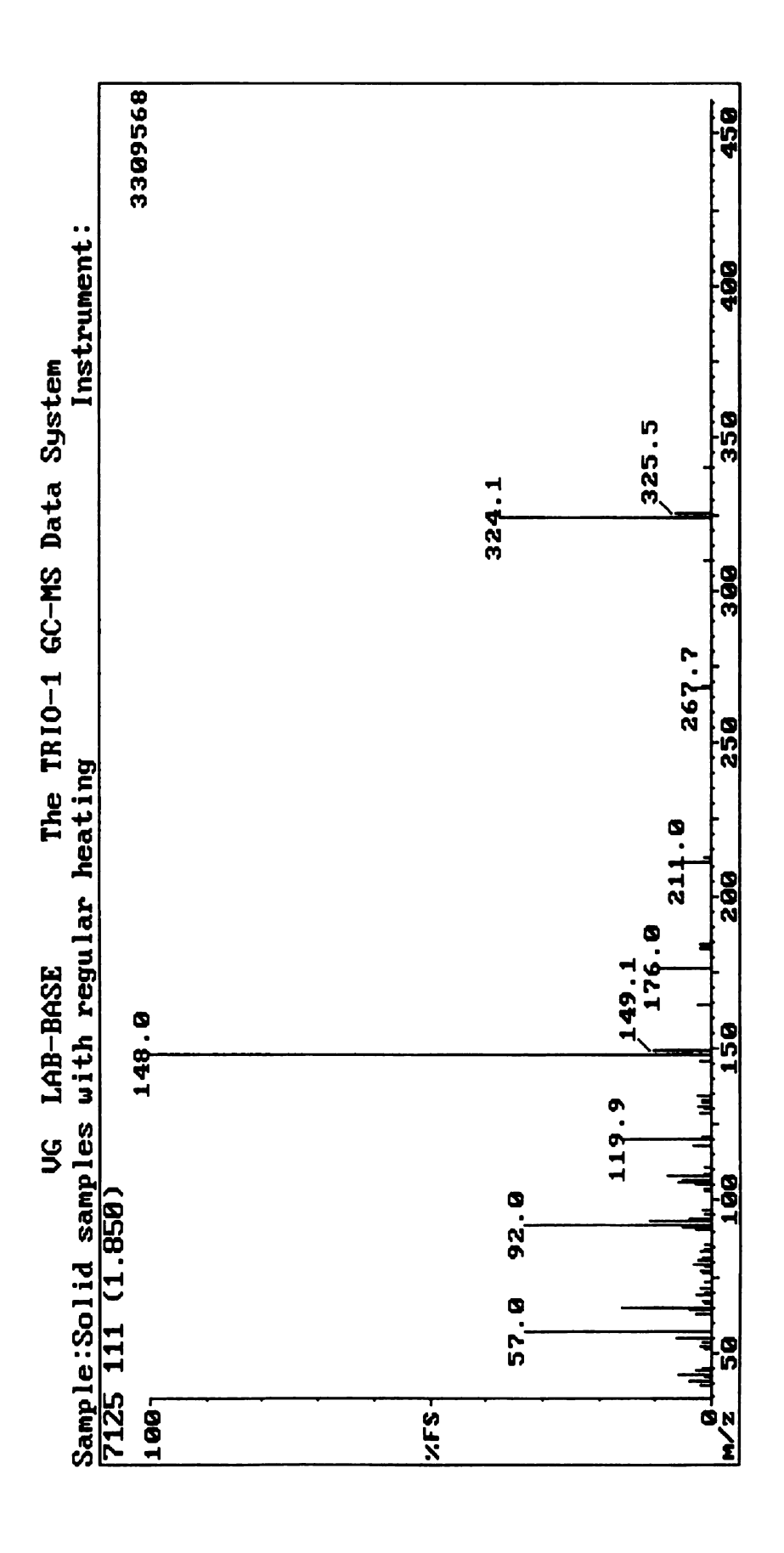
APPENDIX A

MASS SPECTRA OF SYNTHESIZED COMPOUNDS

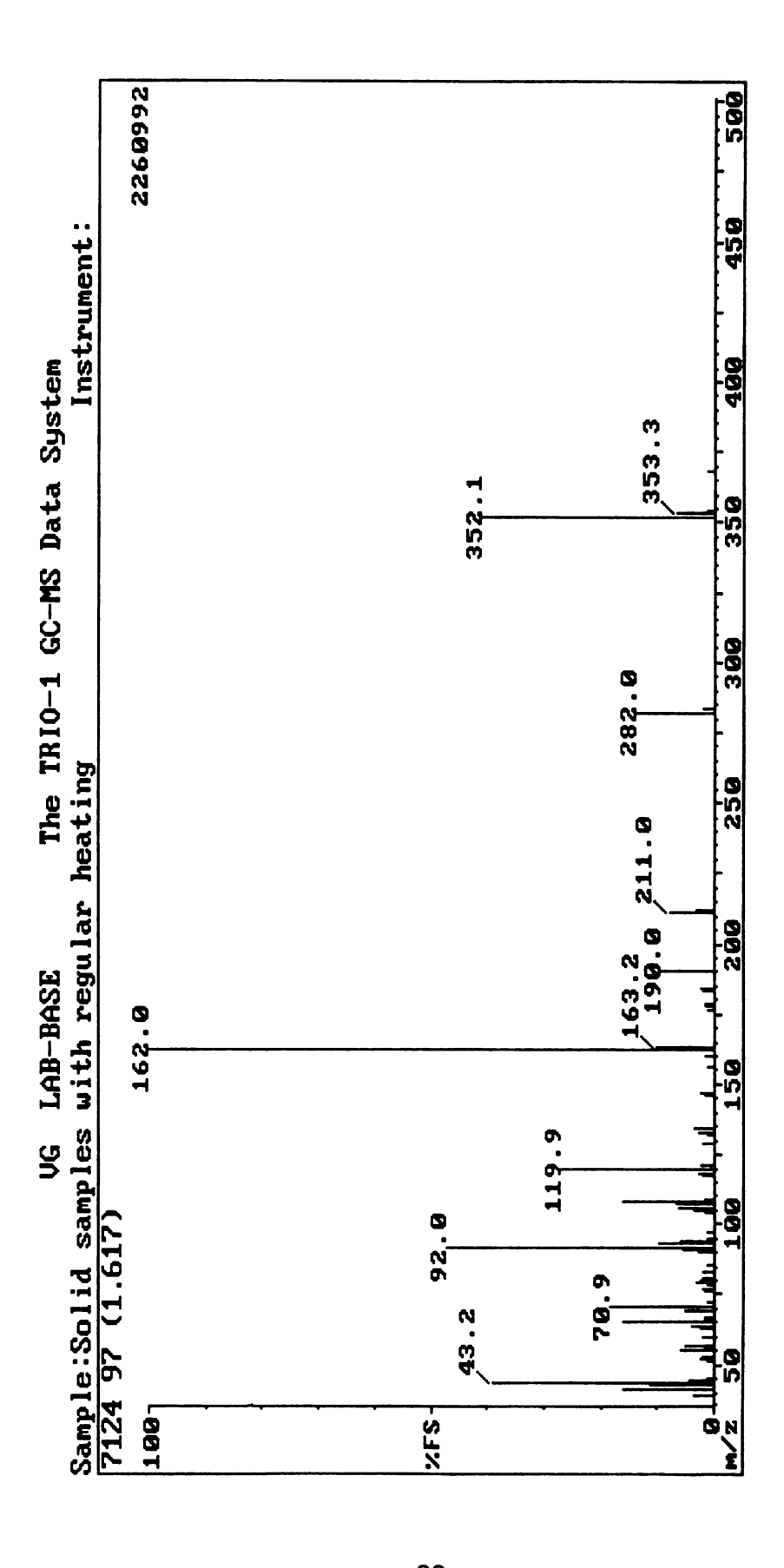
This appendix presents the collected mass spectrum of the synthesized pdiamidoazobenzenes.



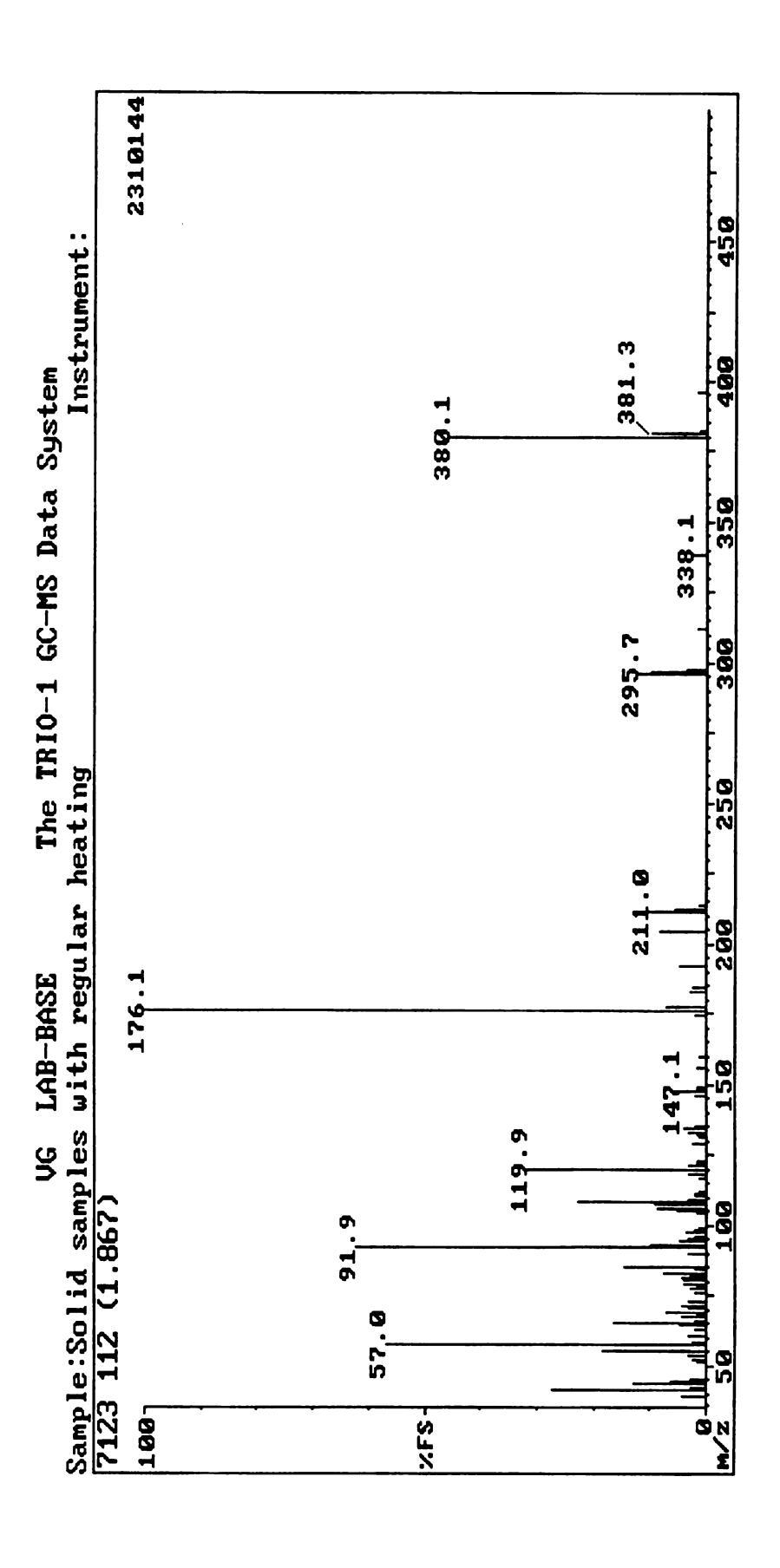
Mass spectrum for compound 1.



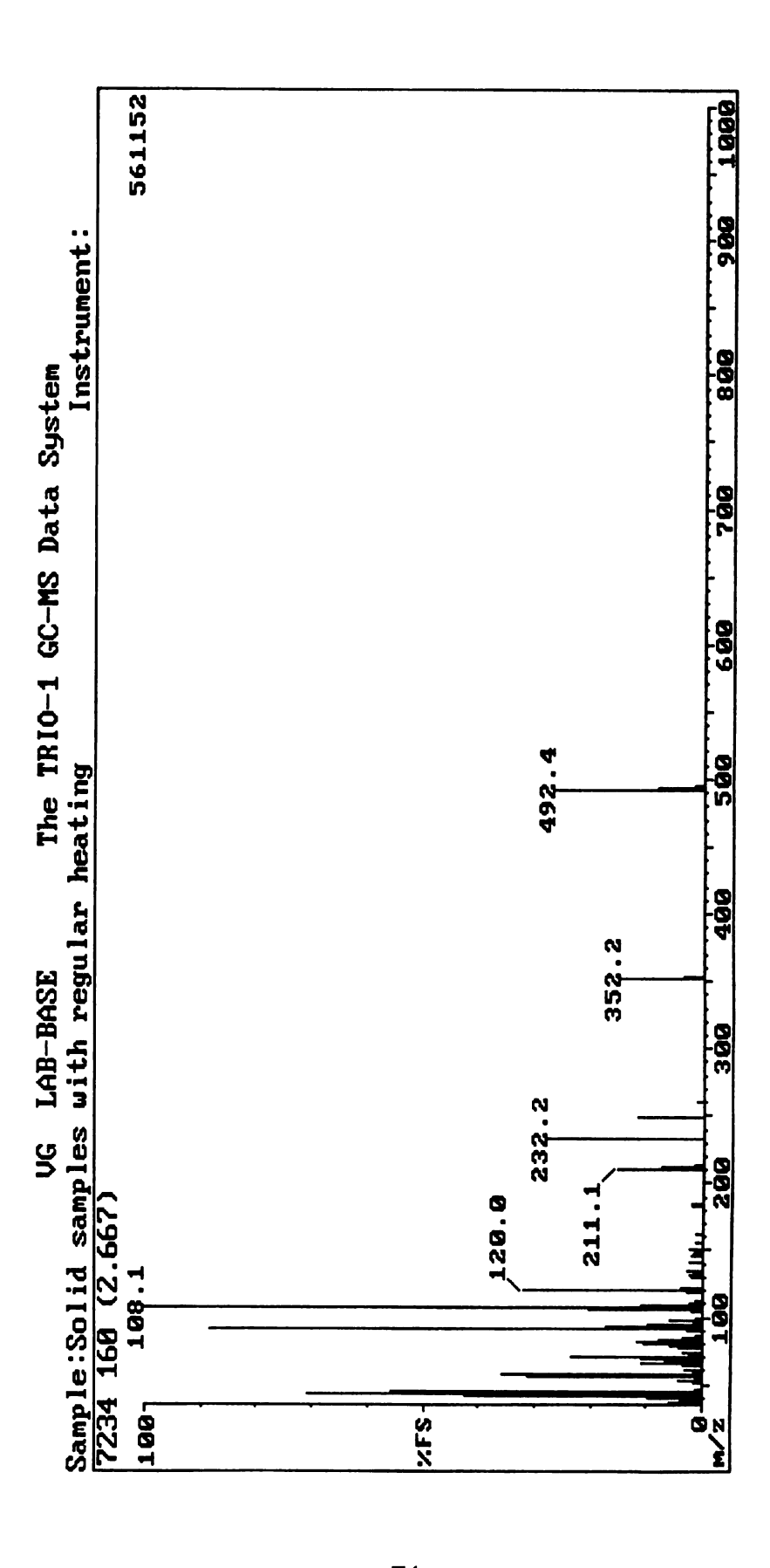
Mass spectrum for compound 2.



Mass spectrum for compound 3.



Mass spectrum for compound 4.



Mass spectrum for compound 5.

